

Acknowledgement

My deepest appreciation goes to my supervisor Hiroyasu Satoh who patiently conducted me throughout this study. I was not able to finish this research without his immense advice, patient guidance, and kind support.

I would like to express equal appreciation to Professor Takashi Mino for his precious comment and valuable advice for complete my research.

I'm equally grateful to my co-supervisor Asso. Prof. Yukio Koibuchi for his valuable comments. I would like to special thank for Prof. Masahiro Hattori and Dr. Kenshiro Oshima laboratory team in the Center for Omics and Bioinformatics, Graduate School of Frontier Sciences for providing technical support. Besides, I express my gratitude to Atsuko Michinaka for her kind advice and encouragement during her stay.

I would like to offer my special thanks to Asian Development Bank – Japan Scholarship Program (ADB-JSP) for support my entire study in Master program in the University of Tokyo.

I'm deeply grateful to my lab-colleagues in Mino/Satoh laboratory, for their great help, kind support when I encountered difficulties. I wish all the best and happiness to my friends Yang He, Su Tao, Shi Wei and Shamsul Huda.

I would like to express my gratitude to secretary Mrs. Takeuchi Yuriko for her kind care during my stay in Japan. Sincere thanks are expressed to Kashiwa International Liaison Office for their great support for my life in Japan.

Finally, I would like to thank my husband Sanchir Ganzorig and my daughter Khuslen Sanchir and my son Amar Sanchir for their encouragement that cheering me up and love that makes me strong.

LIST OF FIGURES

- Figure 2.1 Simple description of enhanced biological phosphorus removal (EBPR) process.
- Figure 2.2 Dissolved contents change in EBPR process
- Figure 2.3 Scheme of the 8 trace element impact analyzing experiments by Yuki Sato (2012)
- Figure 2.4 EBPR performance and trace element content in each Run
- Figure 2.5 Phosphorus removal efficiency of the Run8 (A) and Run10 (B). Yuki Sato, Master thesis 2012)
- Figure 3.1 MLSS concentration of the experiment (Ex) and control (Co) reactors Run_A.
- Figure 3.2 SVI of control and experiment reactor in Run_A
- Figure 3.3 Dissolved organic carbon concentrations in the end of aerobic (Ox) step of experiment (Ex) and control (Co) reactors in Run_A.
- Figure 3.4 Phosphorus concentration in the end of anaerobic (An) and oxidation (Ox) step of experiment (Ex) and control (Co) reactor in Run_A.
- Figure 3.5 MLSS trend in experiment (Ex) and control (Co) reactor in Run_B.
- Figure 3.6. Sludge Volume Index (SVI) trend of the control (Co) and experiment (Ex) reactor in Run_B.
- Figure 3.7 DOC concentration of the Run_B.
- Figure 3.8 Phosphorus concentration in the end of anaerobic (An) and aerobic (Ox) step of experiment (Ex) and control (Co) reactor in Run_B.
- Figure 3.9 Microscope observation of flocculation process in Run_B
- Figure 4.1 Taxonomy assignments of reads at Phylum level of Run8 with PCR and RT-PCR results.
- Figure 4.2 Taxonomy assignments of the reads at Class level of PCR results in Run8
- Figure 4.3 Taxonomy assignments of reads at Class level of RT-PCR results in Run8
- Figure 4.4 Taxonomy assignments of the reads in PCR and RT-PCR result of Run10 in 7 days
- Figure 4.5 Taxonomy assignments of reads in PCR results of Run10
- Figure 4.6 Taxonomy assignments of reads in RT-PCR result of Run10
- Figure 4.7 Partial tree and heatmap distribution of major OTUs in Run8 and Run10.
- Figure 4.8 Extraction heatmap of OTUs related to *Candidatus* 'Accumulibacter Phosphatis'
- Figure 4.9 2D biplot of Accumulibacter related OTUs by PCR results of the Run8 generated by PCA

Figure 4.10 2D biplot of Accumulibacter related OTUs by RT-PCR results of the Run8 generated by PCA

Figure 4.11 2D biplot of Accumulibacter related OTUs in PCR result of the Run10 generated by PCA

Figure 4.12 2D biplot of Accumulibacter related OTUs in RT-PCR result of the Run10 generated by PCA

LIST OF TABLES

Table 3.1 Description of the Runs and trace element concentration

Table 3.2 Carbon, phosphorus and trace element concentrations in influent

Table 4.1 Trace element concentrations added in the influent ($\mu\text{g/L}$)

Table 4.2 Total obtained reads number referred to each days and sample number

LIST OF ACRONYMS

EBPR	Enhanced Biological Phosphorus Removal
bp	basepair
DO	Dissolved oxygen
DOC	Dissolved organic carbon
MLSS	Mixed Liquor Suspended Solids
OTU	Operational Taxonomic Unit
OTUMAMi	Operational Taxonomic Unit Management And Mining
PCR	Polymerase Chain Reaction
QIIME	Quantitative Insight Into Microbial Ecology
RDP	Ribosomal Database Project
RT-PCR	Reverse-transcription Polymerase Chain Reaction
SBR	Sequencing Batch Reactor
SVI	Sludge Volume Index
TOC	Total organic carbon
WWTP	Wastewater treatment plants

TABLE OF CONTENTS

CHAPTER ONE	8
1.1 Introduction	8
1.2 Objectives and Scope	9
1.3 Research framework	9
1.4	10
Structure of Thesis	10
CHAPTER TWO	11
2.1 The Enhanced Biological Phosphorus Removal process.....	11
2.2 Parameters affecting EBPR efficiency	13
2.3 Molecular method to analyze microbial population	14
2.4 Previous research data	16
CHAPTER THREE	19
3.1 Materials and Methods	19
3.1.1 Reactor operation	19
3.1.2 Sampling.....	22
3.1.3 Sample analyses.....	23
3.2 SBR performance result	24
3.2.1 Results of Run_A.....	24
3.2.2 Experiment of Run_B	27
CHAPTER FOUR	31
4.1 Materials and Methods	31

4.1.1	Run8 and Run10 operated by Yuki Sato	31
4.1.2	PCR and Reverse-Transcription PCR (RT-PCR).....	33
4.1.3	Second PCR with barcoded primers.....	34
4.1.4	Pyrosequencing data analysis.....	35
4.2	Pyrosequencing data result	37
4.2.1	Run8.....	38
4.2.2	Run10.....	41
4.2.3	Operational Taxonomic Units (OTUs) of the Run8 and Run10.....	44
4.2.4	OTUs related to <i>Candidatus</i> ‘Accumulibacter Phosphatis’	48
CHAPTER FIVE	53
5.1	Conclusion	53
5.1.1	Reactor operation experiments	53
5.1.2	Microbial community analysis on Run8 and Run10 samples of Yuki Sato	53
5.2	Recommendation	54
5.2.1	Reactor operation experiment.....	54
5.2.2	Microbial community analysis.....	54
Reference:	55
Journal and Article reference:	55
Book reference	58
Website reference	58
Appendices	59
Appendix I	60

CHAPTER ONE

1.1 Introduction

A population growth of the world leads to the increase of demand to safe water. The purpose of wastewater treatment is to remove pollutants from wastewater so that treated water can be reused while the environment of the receiving water bodies is preserved. Nutrients such as nitrogen and phosphorus are often not directly harmful to human health, but can cause pollution problems by stimulating algal bloom and trigger eutrophication in closed water bodies (Sundblad et al., 1994).

In 1914, the “activated sludge” process was developed as a highly effective method to treat wastewater (Lindrea and Seviour, 2002). Since that time, activated sludge process has been dominantly employed to treat urban sewage worldwide. While at the initial stage of the development of the activated sludge process, the target of removal was only biochemical oxygen demand, in the latter stage, removal of nutrients such as nitrogen and phosphorus has been enabled.

Enhanced biological phosphorus removal (EBPR) process, one of the modified activated sludge processes, is dedicated to remove phosphorus from wastewater. It includes anaerobic zone in the biological process to promote proliferation of phosphorus accumulating microorganisms (PAO). While EBPR process is applied to many wastewater treatment plants, the control of EBPR is not easy. The reason of the unstable performance of EBPR is still unclear, however many studies have been done in the last decades about the impact of temperature, pH, nutrient balance, micronutrients, bacteriophage and others.

In the previous study done by Yuki Sato (Sato, 2012), the effects of trace elements on EBPR performance was focused. He examined 8 trace elements (Co, Cu, Fe, Mo, I, Bo, Mn, Zn),

and as a result, he concluded that iron (Fe) is the most responsible for the EBPR efficiency than other trace elements in his laboratory EBPR reactor.

At the same time, validating trace element shortage affect could increase the control ways to keep EBPR system stable.

Culture independent microbial analysis method, which molecular biology techniques extend the understanding of the bacterial community and its behavior. DNA sequencing technology gives advance to recognize bacteria by whole genomes, which was unknown recently. Next-generation DNA sequencing is rapid developing method which enabling brand new approaches to the medical and biological research.

1.2 Objectives and Scope

Based on the study by Sato (Sato, 2012), the author focused on the effects of trace elements especially iron on EBPR in this study. This study was conducted to clarify the relationship between microbial community change and EBPR deterioration due to trace elements shortage. And, reproducibility of the shortage of trace elements especially Fe on EBPR performance is next objective.

1.3 Research framework

To attain above goals, present research consists of two main studies, which are;

- a. Operate two EBPR sequencing batch reactor in parallel and observe the performance
- b. Make microbial community analyses on the samples obtained from of Run8 and Run10 of Yuki Sato (2012), which EBPR performance affected by trace elements shortage

1.4 Structure of Thesis

Thesis consists of 5 chapters as following,

Chapter 1 Briefly described research introduction, objective, its framework and outline of thesis.

Chapter 2 Literature review of a) EBPR process and parameters which affect stable performance, and researches conducted about trace element effect to EBPR process b) microbial community analyzes method based on 16S rRNA gene amplification were summarized. And study of Yuki Sato was briefly described in here and reason to choose Run8 and Run10 samples for microbial community analysis.

Chapter 3 Methodology and results description of 2 Runs on the two lab-scaled EBPR sequencing batch reactors, which Run_A intended to focus on trace element shortage, and Run_B designed to investigate Fe shortage effect on EBPR performance.

Chapter 4 Methodology, sample preparation steps and pyrosequencing result description of the microbial community analyses on the Run8 and Run10 samples of the Yuki Sato, based on 16S rRNA and 16S rDNA pyrosequencing.

Chapter 5 Conclusions of summary of completed work outlined and further research proposals recommended.

CHAPTER TWO

Review of literature

2.1 The Enhanced Biological Phosphorus Removal process

Phosphorus is an essential element for growth of all living organisms. Phosphorus is involved in cellular components such as adenosine triphosphate (ATP), nucleic acids (DNA and RNA) and phospholipids in cell membrane. In natural water environment, phosphorus is often a limiting factor of growth of different organisms, as the amount of biomass is limited by the availability of phosphorus. Excess phosphorus in water bodies can trigger overgrowth of algae and cause eutrophication problems. Some of blue-green algae are known to produce toxins, and during night, they consume oxygen in water. Both the toxic effects and hypoxia threaten aquatic lives. On the other hand, increase of algae in water source causes difficulty in solids removal from raw water. In general, dissolved carbon concentration in raw water is also increased, and chlorine dose for disinfection tends to be increased. To prevent water pollution, controlling P emission to water environment is very important. The source of P emission is often divided into two: non-point sources and point sources. It is difficult to remove P emitted from non-point sources such as agricultural run off, and often cost effective countermeasures are to remove P in wastewater at wastewater treatment plants.

Phosphorus in domestic wastewater is in a range of 4 – 12 mgP/L (Metcalf & Eddy, Wastewater engineering, 2004) and can be removed by chemical and biological methods. Chemical precipitation methods are reliable, but the cost for chemicals should be considered, and it also causes an increase in sludge generation. On the other hand, the enhanced biological phosphorus removal process (EBPR) is a representative biological method to remove phosphorus from wastewater. It does not require chemicals, is also known to be effective to control bulking, and P content in excess sludge will be increased. The last point is of importance because it can lead to the recovery and reuse of P for fertilizer. Based on these advantages, the EBPR process is considered as an economical and environment-friendly biotechnology to treat wastewater.

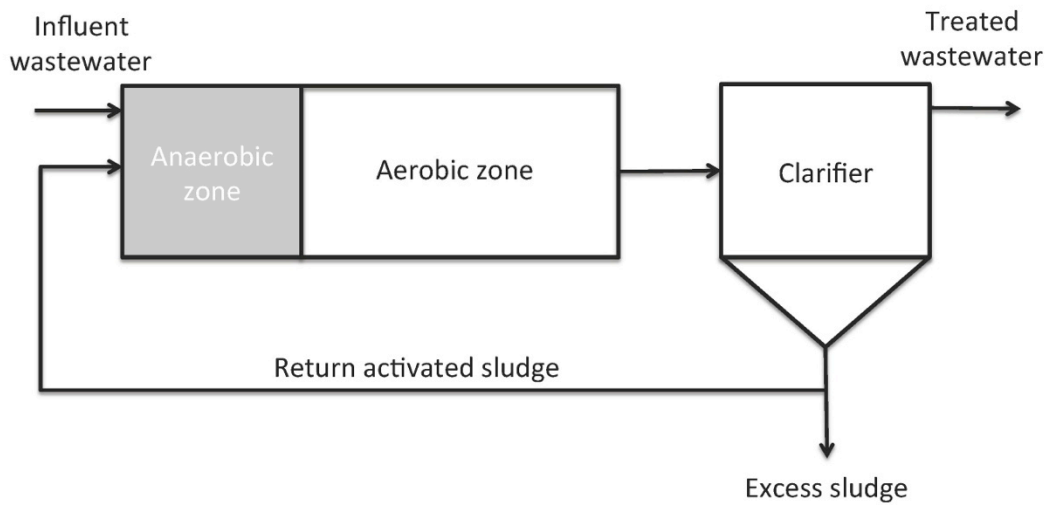


Figure 2.1 Simple description of enhanced biological phosphorus removal (EBPR) process.

EBPR process was discovered unintentionally. It was found that that activated sludge can take up high dose of phosphorus than microbial growth requirement in plug flow activated sludge plants. The EBPR process has 2 zones, anaerobic zone and aerobic zone (Barnard et al., 1975). In the anaerobic zone, polyphosphate accumulating organisms (PAOs) take up organic matters while releasing phosphorus. In the aerobic zone, they absorb phosphate in the supernatant and convert it to polyphosphate in their cells. At the end of the aerobic zone, phosphate concentration is much lower than that in the influent (Mino et al., 1998). Then activated sludge and treated water are separated at the secondary settling tank, and most of polyphosphate-rich activated sludge is returned to the anaerobic zone. And small amount of polyphosphate-rich activated sludge is removed from the system as excess sludge, and sent to sludge treatment.

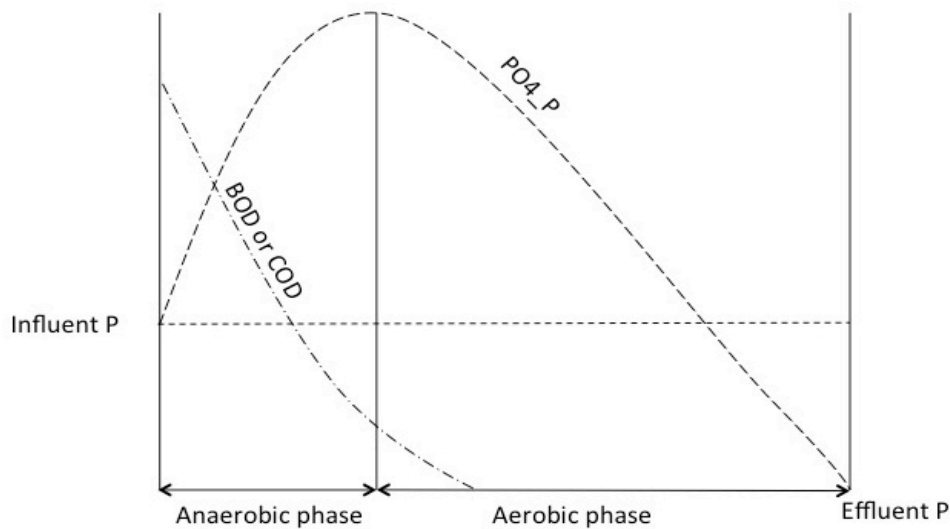


Figure 2.2 Dissolved contents change in EBPR process

In more detail, in the anaerobic phase, returned active sludge and wastewater are mixed. Here PAOs absorb organic substrates such as volatile fatty acids (VFAs) in the wastewater and store them in their cells in such forms as polyhydroxyalkanoates (PHAs) typically composed of 3-hydroxybutyrate (3HB) and 3-hydroxyvalerate (3HV) (Sato et al., 1992). To take up organic substrates, PAOs use polyphosphate stored in their cells as the source of energy. When these intracellular polyphosphate is hydrolyzed, orthophosphate is formed and released into the supernatant (Figure 2.2). In the following aerobic phase, PAOs oxidative utilize stored PHAs, and generates energy. Some part of the generated energy is utilized to regenerate intracellular polyphosphate: the generation of polyphosphate is accompanied by the uptake of orthophosphate in the supernatant into their cells (Mino et al., 1998). More orthophosphate is taken up into cells than they were released in previous anaerobic phase. As a result, phosphate in the bulk liquid (wastewater) is moved into biomass, which will finally be removed from the wastewater treatment system with excess sludge.

2.2 Parameters affecting EBPR efficiency

However EBPR system widely applied to wastewater treatment plants, still challenging unstable performance. Thus, treatment plants use chemical precipitation for backup reason. Many factors can affect to the EBPR, but one of the major reasons is phosphorus accumulating organism and glycogen accumulating organisms (PAO-GAO) competition (Sato et al., 1994). They compete with PAO for organic carbon substrate and do not

contribute to remove phosphorus from wastewater (Seviour et al., 2010). Second main reason of EBPR process deterioration is filamentous bacterial proliferation and leads to bulking and foaming (Tandoi et al., 2006). Mostly PAOs favor in cool temperature up to 20⁰C than GAOs which proliferate in higher temperature around 30⁰C, that's why EBPR plant failure common in summer (Lopez-Vazquez et al., 2008). Little fluctuation of pH (in range from 7.2 to 6.3) affected EBPR performance, thus keep pH neutral helps to maintain operation stable (Converti et al., 1995, Liu et al., 1996). Sludge Retention Time set to 9–13 days during the winter and 5–7 days during summer helped to keep stable EBPR reported by Oldham and Rabinowitz (2002). The availability of carbon source is another impact. Schuler and Jenkins (2003) reported Phosphorus/acetate-COD ratio approximately 0.12 would achieve high P removals. Favorable Dissolved oxygen (DO) concentration is 2 mg/L for successful biological P removal (Shehab et al., 1996). Above-mentioned parameters failure would trigger EBPR loss or unstable performance. Less nutrient wastewater such as industrial wastewater need micronutrient for improve treatment efficiency (Burgess et al., 1999).

Identification and isolation of the PAOs is very difficult, and even now, the typical PAO has not yet been isolated. Major PAOs participating in EBPR under different conditions are still unknown (Oehmen et al., 2007). Despite difficulties of the isolation of PAOs, several of them have been found to participate in full-scale and laboratory-scale EBPR processes through culture independent molecular techniques, such as 16S rRNA based clone library and fluorescent in situ hybridization (FISH) etc. *Candidatus* 'Accumulibacter Phosphatis', an uncultured *Rhodocyclus* -related Betaproteobacteria organism, has been reported as the dominant PAO in laboratory-scale acetate-fed reactors (Bond et al., 1995, Hesselmann et al., 1999, Crocetti et al., 2000) and in conventional full-scale treatment plants (Zilles et al., 2002; Kong et al., 2004). Until recently, still all attempts have failed to culture this bacterium, however can be enriched in the lab-scaled reactors.

2.3 Molecular method to analyze microbial population

A few decades ago, bacterial analysis in environmental samples and wastewater was based on culture method, in which target bacteria is isolated and grown in laboratory to analyze its physiological characteristics. But now, culture-independent methods so called molecular

analyses methods are widely used (Amann et al., 1995). In many of molecular methods, phylogenetic identification is performed by analyzing 16S rRNA gene sequencing.

When a cell grows, it produces proteins. To produce proteins, information in DNA is transcribed to messenger RNA, and the sequence of messenger RNA is translated into amino acid sequence. The translation is done by an intracellular organ named ribosome. Ribosome is composed of ribosomal RNA and other catalytic proteins, and is physically separated into two parts, 30S subunit (SSU) and 50S subunit. Each subunit has its own specific ribosomal RNAs and ribosomal proteins. 30S subunit contains 16S rRNA, while 50S subunit has 5S and 23S rRNA (Madigan et al., Brock biology of microorganisms). In 30S subunit has either 16S rRNA molecule for prokaryotes or 18S rRNA for eukaryotes. All living organisms have to produce protein, and thus all living organisms have ribosomes with the same function with similar structures. Thus, sequences of 16S rRNA and 18S rRNA from different organisms have similarities and dissimilarities. Due to these advantages, its sequence is now widely used for phylogenetic classification of microorganisms. The 16S rRNA sequences are now deposited in such databases as GeneBank, Ribosomal Database Project, and so on. Nowadays researchers extract and sequence 16S rRNA gene and compare this sequence to the GeneBank sequence and identify bacterial species. While 16S rRNA is an RNA molecule, its original sequence is found in DNA as 16S rRNA gene.

Polymerase chain reaction (PCR) technique is used to amplify a specific region of DNA. On the other hand, in reverse-transcription PCR (RT-PCR), target region of RNA molecule is reverse-transcribed to DNA, then the target region in DNA molecule is amplified. DNA is known to be stable, and it is considered that detection of 16S rRNA gene by PCR can also detect DNA from dead cells. On the other hand, ribosomes are thought to be more rapidly degraded in dead cells, and its abundance is thought to be related with the rate of protein synthesis. Several studies made both on DNA and RNA in order to compare existing and active cells (of same species) in the sample due to metabolic active cells transcribe more rRNA than inactive cells (Yoshikazu et al., 2003, Boon et al., 2003) and DNA and RNA based comparison can give different species result from same sample (Anderson et al., 2008). 16S rRNA gene (DNA) and 16S rRNA (RNA) amplification method showed different results on same sample, which can be good indicator of bacterial community activities (Sage et al., 2010).

Sanger sequencing is the first DNA sequencing technology, which developed in early 1990's. Shotgun sequencing technology developed in scope of Human Genome Project in order to sequence longer sections of DNA. This technique split or broke DNA into smaller fragments and make sequence on it. Great achievement of this technology is made sequencing entire human genome possible. Next generation sequencing core principle adopted from shotgun sequencing, which is massive parallel sequencing. Function of NGS is, split or broke DNA into small pieces, then connect these small pieces into designated adapters and read randomly during synthesis process. It is novel technique that enabled rapid sequencing of large strains of DNA base pairs of entire genomes and producing hundreds of gigabases of data in a single sequencing run (Shendure and Ji, 2008, Zhang et al., 2011).

2.4 Previous research data

Yuki Sato in his master thesis "*The study on deterioration of biological phosphorus removal without trace element and specification of short trace element*", at Socio-cultural Environmental Studies, Graduate School of Frontier Sciences, The University of Tokyo, 2012, operated two lab-scale activated sludge sequencing batch reactors in parallel to clarify the impact of trace elements on EBPR performance. That is, the two reactors were operated under the identical condition basically with synthetic wastewater with the same compositions containing eight trace elements. And during a fixed period, some or all of trace elements in the feed to one of the reactor (experiment reactor) was omitted, while another reactor was operated as the control under the normal condition.

In Runs 1 to 4, he omitted all the trace elements in the feed, and he always found that EBPR was deteriorated in the experiment reactor immediately after trace elements were omitted. Then he conducted a series of experiments shown in Fig. 2.3 and Table 2.4 to identify the key element which is related with the deterioration of EBPR. First, the 8 trace elements were divided into 2 subgroups, and conducted Run5 and Run6 and found that the reactor fed with Fe, Mo, Cu, and Co but omitted with Mn, Zn, B and I maintained EBPR. On the other hand, in Run 5 when B, I, Mn and Zn were geded but not Fe, Mo, Cu and Co, EBPR was deteriorated. Then, he further conducted Run7 and Run8, and he found that the reactor fed with Fe and Mo but omitted with Cu, Co, B, I, Mn and Zn maintained effective EBPR, but the reactor fed with Cu and Co but omitted with Cu, Co, B, I, Mn and Zn resulted in deterioration of EBPR (Fig.

2.5 A). Further, in Runs 9 he fed to his reactor Fe only but not other 7 elements, and he found EBPR was maintained, though a little bit deteriorated. On the other hand, when he fed to his reactor Mo only in Run 10, EBPR was apparently deteriorated (Fig. 2.5 B).

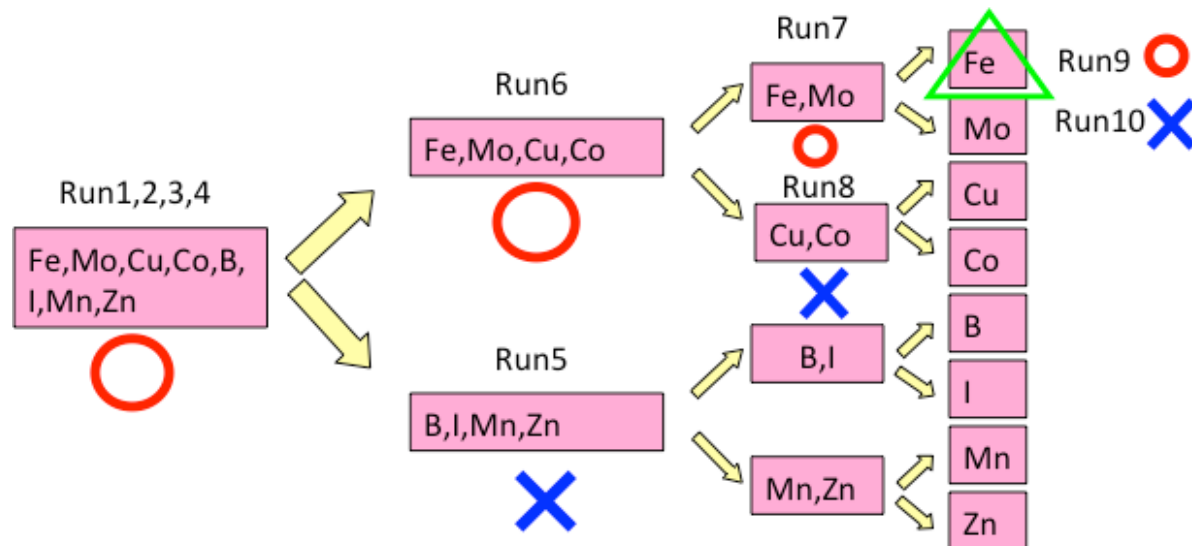


Figure 2.3 Scheme of the 8 trace element impact analyzing experiments by Yuki Sato (2012)

Run	Experiment reactor	EBPR performance	Control reactor	EBPR performance
Run1	Fe, Mo, Cu, Co, B, I, Mn, Zn	Bad	Fe, Mo, Cu, Co, B, I, Mn, Zn	Good
Run2	Fe, Mo, Cu, Co, B, I, Mn, Zn	Bad		
Run3	Fe, Mo, Cu, Co, B, I, Mn, Zn	Bad		
Run4	Fe, Mo, Cu, Co, B, I, Mn, Zn	Good/Bad		
Run5	Fe, Mo, Cu, Co, B, I, Mn, Zn	Bad		
Run6	Fe, Mo, Cu, Co, B, I, Mn, Zn	Good		
Run7	Fe, Mo, Cu, Co, B, I, Mn, Zn	Good		
Run8	Fe, Mo, Cu, Co, B, I, Mn, Zn	Bad		
Run9	Fe, Mo, Cu, Co, B, I, Mn, Zn	Good		
Run10	Fe, Mo, Cu, Co, B, I, Mn, Zn	Bad		

Figure 2.4 EBPR performance and trace element content in each Run

Final result showed that, Fe is the most responsible element out of the 8 trace elements in his EBPR system.

Figure 2.5 shows results of Run 8 and Run 10 in his experiments. In Run8, performance of the control reactor was good throughout the experiment, as can be seen by the low concentration levels of PO₄-P at the end of aerobic phase. On the other hand, EBPR performance in the experiment reactor was deteriorated after trace elements of Fe, Mo, B, I, Mn and Zn were omitted. Similar observation was obtained in Run 10, which was conducted in the same way as in Run 8, but the omitted elements in the experiment reactor were Fe, Cu, Co, B, I, Mn and Zn.

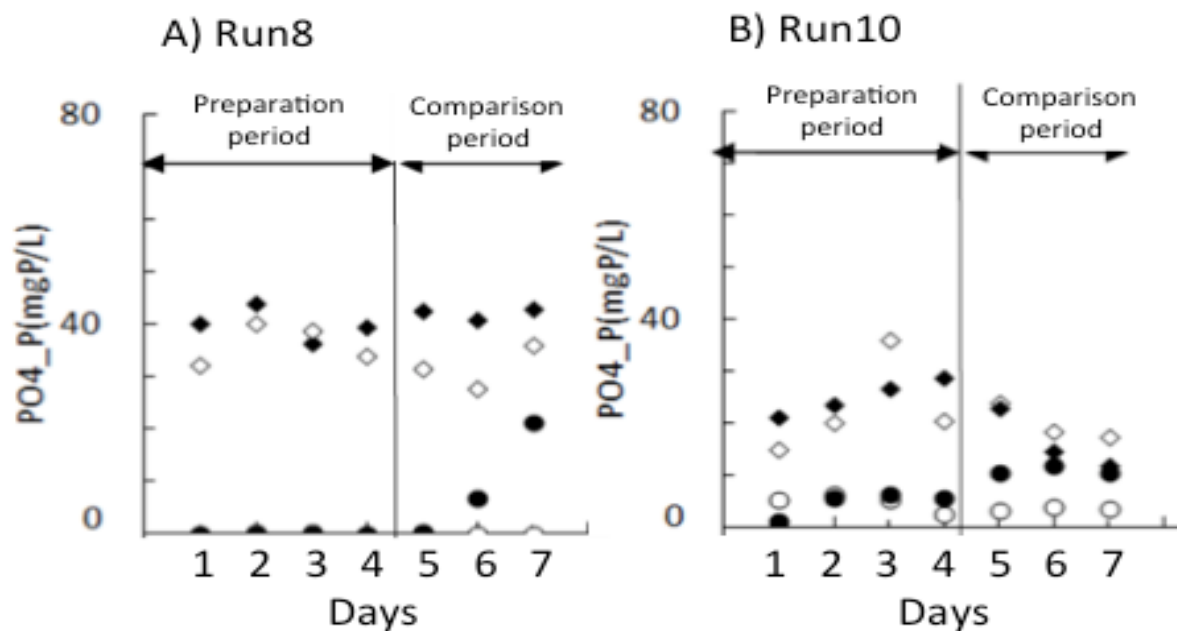


Figure 2.5 Phosphorus removal efficiency of the Run8 (A) and Run10 (B). Yuki Sato, Master thesis 2012)

*Detailed performance of Run8 and Run10 shown in Appendix II.

CHAPTER THREE

Reactor operation experiments

Lab-scaled two sequencing batch activated sludge reactors (SBRs) were operated with synthetic wastewater in parallel. The reactors were operated with sequencing anaerobic and aerobic conditions for enhanced biological phosphorus removal (EBPR). Total two runs (Run_A, Run_B) were performed with these parallel reactors: Run_A was intended to confirm effect of omission of trace element solution in the feed, and Run_B was focused on the effect of omission of Fe.

3.1 Materials and Methods

3.1.1 Reactor operation

Two sequencing batch reactors with a working volume of each 10L were operated in parallel. Two sets of experiments, Run_A and Run_B were conducted to see the effects of omission of trace elements. In Run_A and Run_B, two SBRs (an experiment reactor and a control reactor) were operated under the same condition during initial 6 days as “preparatory period”. Then, feed for the experiment reactors were replaced with feed which lacks target trace element(s), and operation was continued as “comparison period”. The SBRs were operated as follows.

Each of the cycles was 4 hours; 1 hour anaerobic including feeding at the initial several minutes, 2 hours aerobic and 1 hour for settling and discharge of treated water. Sludge retention time (SRT) was set to around 7 days by discharging excess sludge in every cycle and hydraulic retention time (HRT) was 8 hours by discharging 5L effluent, adding same volume synthetic wastewater.

At the beginning of each cycle, 5 L synthetic wastewater was added to the reactor per cycle with addition of 50mL each of stock carbon solution and stock phosphorus solution, respectively.

The stock carbon solution was prepared by dissolving following components in 5L of tap water: sodium acetate trihydrate ($\text{CH}_3\text{COONa}\cdot 3\text{H}_2\text{O}$) – 56.5g, sodium propionate ($\text{CH}_3\text{CH}_2\text{COONa}$) – 28.5g, peptone – 50g, yeast extract – 10g, KCl – 21g, $\text{CaCl}_2\cdot 2\text{H}_2\text{O}$ – 6.6g, $\text{MgSO}_4\cdot 7\text{H}_2\text{O}$ – 55g. The stock carbon solution was autoclaved.

Stock phosphorus solution was prepared by dissolving 76g of K_2HPO_4 and 150 mL of stock trace element solution in 10L of tap water.

Stock trace elements solution was prepared by dissolving in 1L of reverse osmosis water $\text{FeCl}_3\cdot 6\text{H}_2\text{O}$ - 3750mg/L, H_3BO_3 - 375mg/L, $\text{CuSO}_4\cdot 5\text{H}_2\text{O}$ - 75mg/L, KI - 450mg/L, $\text{MnCl}_2\cdot 4\text{H}_2\text{O}$ - 300mg/L, $\text{Na}_2\text{MoO}_4\cdot 2\text{H}_2\text{O}$ - 150mg/L, $\text{ZnSO}_4\cdot 7\text{H}_2\text{O}$ - 300mg/L, $\text{CoCl}_2\cdot 6\text{H}_2\text{O}$ - 375mg/L, EDTA - 25000mg/L. However, stock trace element solution was omitted in the feed for the experiment reactor in Run_A during the comparison period, and the stock trace element solution for the experiment reactor in Run_B during the comparison period was omitted with iron ($\text{FeCl}_3\cdot 6\text{H}_2\text{O}$) in order to create Fe shortage condition.

Influent trace element content referred to each Runs and experiment described in Table 3.1.

In each cycle at the beginning of the cycle, 50mL of stock carbon solution, 50mL of stock phosphorus solution, and 4.9L of tap water was supplied to the reactor, making the concentrations of carbon, phosphorus and trace element concentrations in synthetic wastewater as shown in Table. 3.2.

The SBRs were install in an air-conditioned room at around 20° C. The hydraulic retention time was 8 hours, as each cycle was 4 hours and in each cycle 5L of water was replaced. At the end of the anaerobic and aerobic phases, 150 mL of the mixed liquor was withdrawn to maintain the sludge retention time to be 7 days.

Dissolved oxygen (DO) was measured by a DO meter (DO-21P, DKK-TOA, Japan), and controlled in a range between 2.3 - 2.5 mg/L by a monitoring and control software developed on LabView 8.6. pH was monitored by a pH meter (WM-22EP, DKK-TOA, Japan) and the values were logged by the software.

Table 3.1. Description of the Runs and trace element concentration

Trace elements	Run_A			Run_B		
	Preparatory period (Days 1-4)	Comparison period (Days 5-7)		Preparatory period (Days 1-4)	Comparison period (Days 5-7)	
	Both Control and Experimental Reactors ($\mu\text{g/L}$)	Control Reactor ($\mu\text{g/L}$)	Experimental Reactor ($\mu\text{g/L}$)	Both Control and Experimental Reactors ($\mu\text{g/L}$)	Control Reactor ($\mu\text{g/L}$)	Experimental Reactor ($\mu\text{g/L}$)
Fe	56.9	56.9		56.9	56.9	
B	4.8	4.8		4.8	4.8	4.8
Cu	1.4	1.4		1.4	1.4	1.4
I	25.3	25.3		25.3	25.3	25.3
Mn	6.5	6.5		6.5	6.5	6.5
Mo	4.4	4.4		4.4	4.4	4.4
Zn	5.0	5.0		5.0	5.0	5.0
Co	8.2	8.2		8.2	8.2	8.2

The operational conditions were basically the same as that Sato (2012) used, except trace element concentration in influent is 0.6 times lower than Sato experiment.

The seed sludge was obtained from a local activated sludge wastewater treatment plant on Feb. 27, 2013. Then, the sludge was acclimatized in two SBRs. The operation of the two SBRs were started on March 6th, 2013 with the feed as has been described above. On April 4, sludge in the two SBRs were mixed, divided into two, and returned to the two SBRs. Then, Run_A was started.

Run_B was started with excess sludge collected from Run_A. Two SBRs were inoculated with excess sludge from Run_A on April 25th, 2013, and both of the reactors were operated under the conditions described above. Then, on May 2nd, activated sludge in the two reactors were mixed, divided into two, and returned to the reactors. Then, Run_B was operated from May 2nd to 16th.

Each reactor operations continued 14-16 days. After 6-7 days, in Run_A, experiment reactor stock P substrate changed by new one, which no trace element added. In the Run_B, after 7 days, stock P substrate changed by new substrate which special trace element solution added. Trace element solution of Run_B described below.

Table 3.2. Carbon, phosphorus and trace element concentrations in influent

Components	Concentration
Organic carbon	90.99 mgC/L
Phosphorus	12.58 mgP/L
Fe ^{*,**}	56.9
B ^{**}	4.8
Cu ^{**}	1.4
I ^{**}	25.3
Mn ^{**}	6.5
Mo ^{**}	4.4
Zn ^{**}	5.0
Co ^{**}	8.2

* In Run_B in the feed for the experiment reactor, FeCl₃·6H₂O was omitted during the comparison period.

** In Run_A in the feed for the experiment reactor, trace element solution was omitted during the comparison period.

3.1.2 Sampling

Sampling for Dissolved organic carbon (DOC), PO₄-P, mixed liquor suspended solids, sludge volume index, and microbial analysis were made every another day. Samples for DOC and PO₄-P determination were taken at the end of anaerobic and end of aerobic phases of one

cycle in selected sampling day. Samples for MLSS, SVI and microbial analysis were taken at the end of an aerobic phase. Samples were taken from both experiment and control reactors simultaneously.

Samples for DOC and PO₄-P analyses were directly filtered through 0.45 µm Cellulose Acetate filter (Advantec Inc.), then 25mL of the filtrate was stored for TOC measurement and 1mL for PO₄-P measurement.

For the determination of MLSS, 50mL of activated sludge mixed liquor was taken, centrifuged for 5 minutes at 3,500 rpm, discarded the supernatant, added 50mL RO water and centrifuged again 5 minutes, discarded supernatant and remained samples were used to measure the MLSS.

3.1.3 Sample analyses

The concentration of MLSS is test for suspended solids in mixed liquor, and was determined according to Standard Methods (APHA, 2005). After washing and drying in the room temperature, dishes dried in the drying oven for 2 hours or more at 108⁰C and allowed to cool in the desiccator at least 30 minutes, then measure the weight (A) of the empty dishes. Samples dried and cooled in same way as dishes then scale the weight (B). Then calculated difference in empty and sample added dishes mass as following equation,

$$MLSS = \frac{(B - A) * 1000}{Volume\ of\ sample}$$

In here, B – dish weight with sample, A – empty dish weight and volume of sample – 25mL in this study.

Sludge volume index (SVI) was measured according to Standard Methods (APHA 2005). Activated sludge mixed liquor of 100 mL was taken from a reactor and observed the volume of settled sludge bed after 30 minutes. SVI was calculated as following equation.

$$SVI\ (mL/g) = \frac{Volume\ of\ settled\ sludge\ \left(\frac{mL}{L}\right) * 1000}{MLSS\ \left(\frac{mg}{L}\right)}$$

In some cases, microscope observation for flocculation has done by Microscope.

Concentration of dissolved organic carbon (DOC) was measured by a TOC analyzer (TOC-VCSN, Shimadzu, Japan).

The concentration of PO₄-P was determined by an ICS-3000 ion chromatograph with an AS12A column and an ASRS suppressor (Dionex). Carbonate buffer solution (containing 2.7mM sodium bicarbonate and 0.3mM sodium carbonate) was used as the eluent at a flow rate of 1.5mL/min. Anion standard mixture solution from Kishida Chemicals Inc., Japan, was used as the standard.

3.2 SBR performance result

With the parallel two SBRs, 2 runs of experiments were conducted. Run_A was conducted to examine the reproducibility of EBPR deterioration when trace elements in the influent synthetic wastewater was omitted. In Run_B, the effect of omission of Fe was focused.

3.2.1 Results of Run_A

The results of Run_A were as shown in Figs. 4.1~4.4..

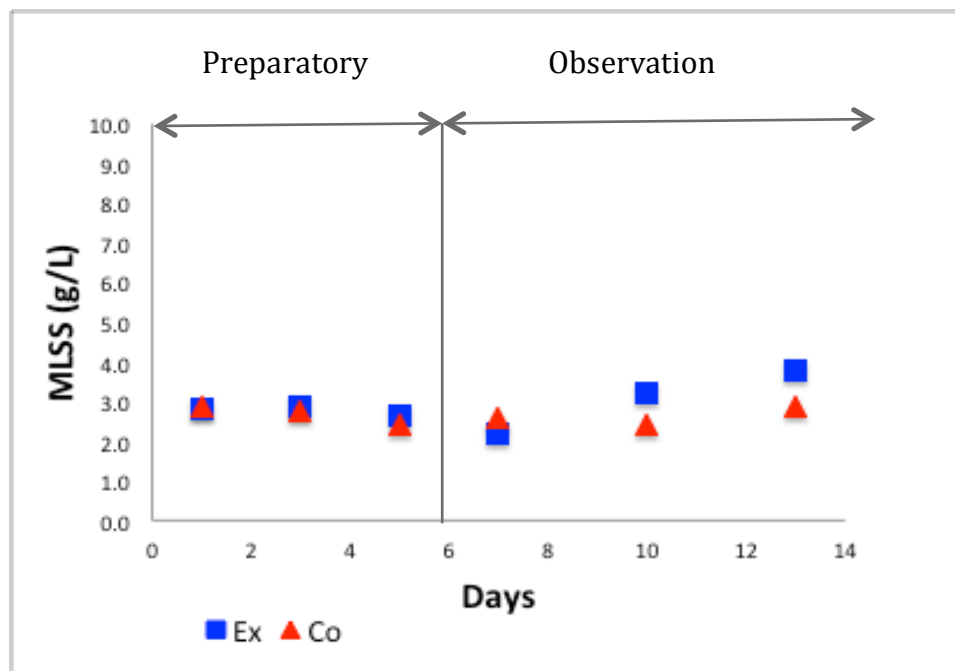


Figure 3.1 MLSS concentration of the experiment (Ex) and control (Co) reactors Run_A.

As shown in Fig. 3.1, MLSS of experiment and control reactor both around 2.0 – 3.0 g/L before stopped trace element supply. Then experiment reactor MLSS increased a little up to 4.0 g/L from 10th day. Typical control amount of MLSS is 2 – 4 g/L (Metcalf & Eddy. Wastewater engineering, p.814).

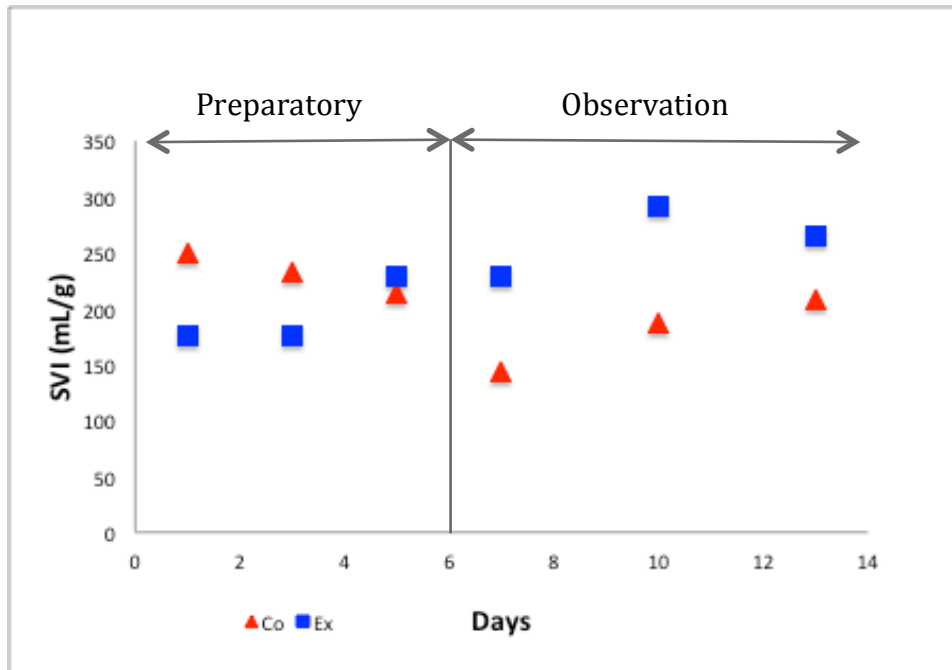


Figure 3.2 SVI of control and experiment reactor in Run_A

As shown in Fig. 3.2, control reactor SVI was around 250 mL/g, then gradually decreased until 150 mL/g, then increased up to 200 mL/g. SVI of the experiment reactor was 180 mL/g initially, then around 230 mL/g when condition changed. After that, increased up to 292 mL/g then decreased to 264 mL/g which could be bulking occurred. Basically in Run8, both reactor SVI was higher than 150 mL/g which could be occurred due to temperature increase (Krishna and van Loosdrecht, 1999).

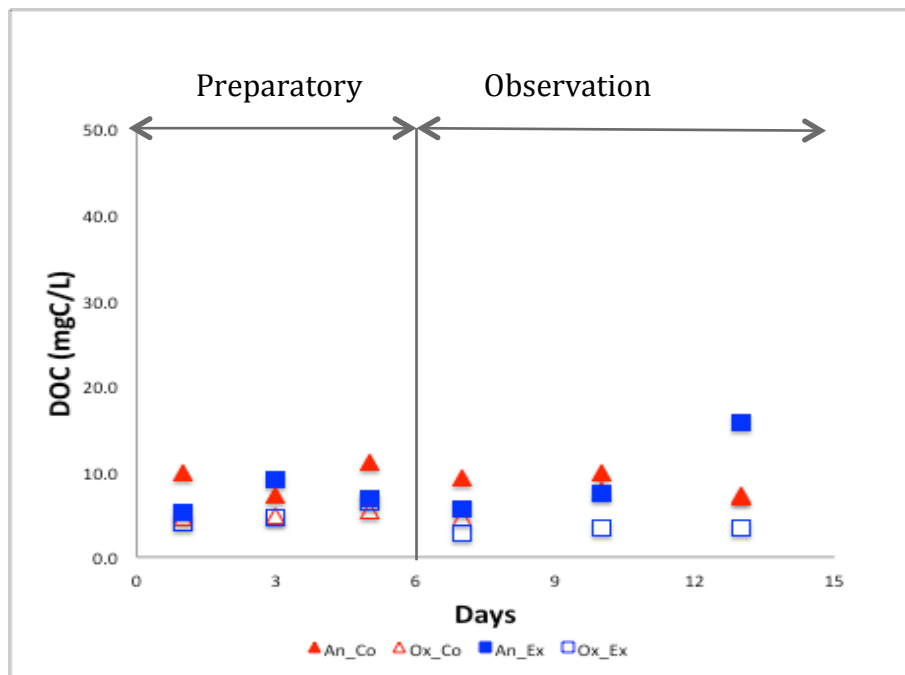


Figure 3.3 Dissolved organic carbon concentrations in the end of aerobic (Ox) step of experiment (Ex) and control (Co) reactors in Run_A.

Figure 3.3 shows DOC concentration in the end of aerobic (Ox) phase of experiment (Ex) and control (Co) reactors. Carbon removal was stable, but experiment reactor carbon removal was improved after condition changed, compare to control reactor.

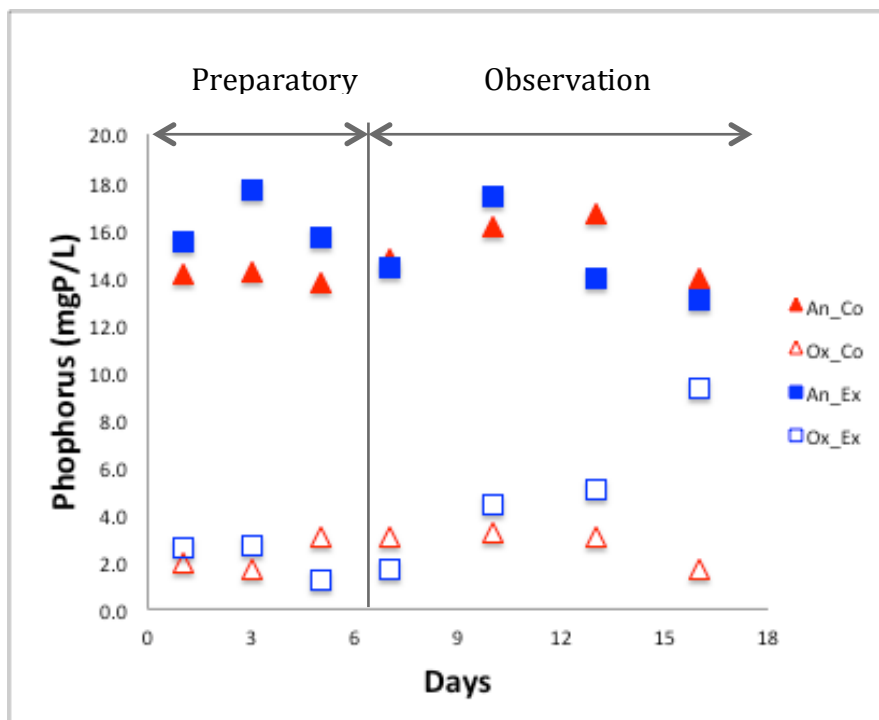


Figure 3.4 Phosphorus concentration in the end of anaerobic (An) and oxidation (Ox) step of experiment (Ex) and control (Co) reactor in Run_A.

In Fig. 3.4, P concentration of the experiment (Ex) and (Co) control reactor in the end of anaerobic (An) and aerobic (Ox) phase. Upper trend shows P release, lower trends shows P uptake capacity of the microorganisms in the EBPR system. In other words, lower trend shows effluent P concentration and increase means P removal deteriorated. As shown in Figure 3.4, deterioration of phosphorus removal was observed in the experiment reactor, since omission of trace elements, which from day 10th effluent P concentration (□ Ox_Ex) gradually increased. On day 16th, or about 10 days after condition changed, effluent concentration sharply increased which showed P removal deterioration. At the same time, control reactor phosphorus removal was not deteriorated. Both reactor operation conditions were same, except experiment reactor stopped to feed by trace elements.

3.2.2 Experiment of Run_B

Figure 3.5 – 3.9 shows Run_B performance.

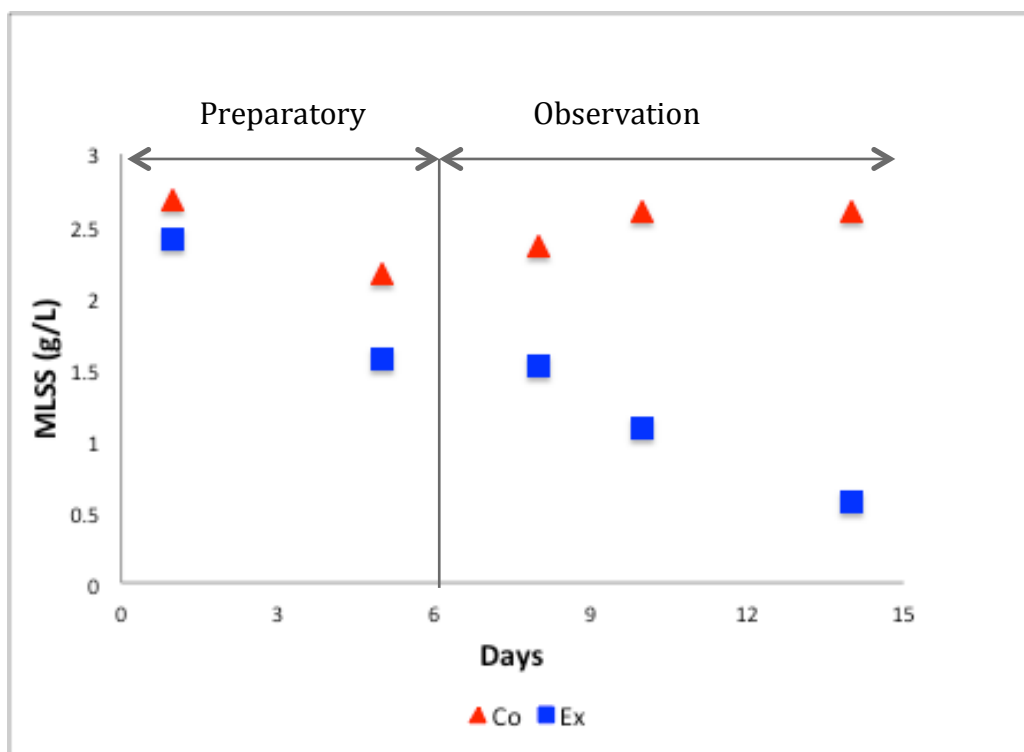


Figure 3.5 MLSS trend in experiment (Ex) and control (Co) reactor in Run_B.

As shown in Figure 3.5, experiment reactor MLSS gradually dropped and last 14th day it reached 0.5 g/L indicated biomass gradually removed from the reactor and biological treatment eliminated (Shehab et al., 1996). Control reactor MLSS was kept around 2.5 g/L.

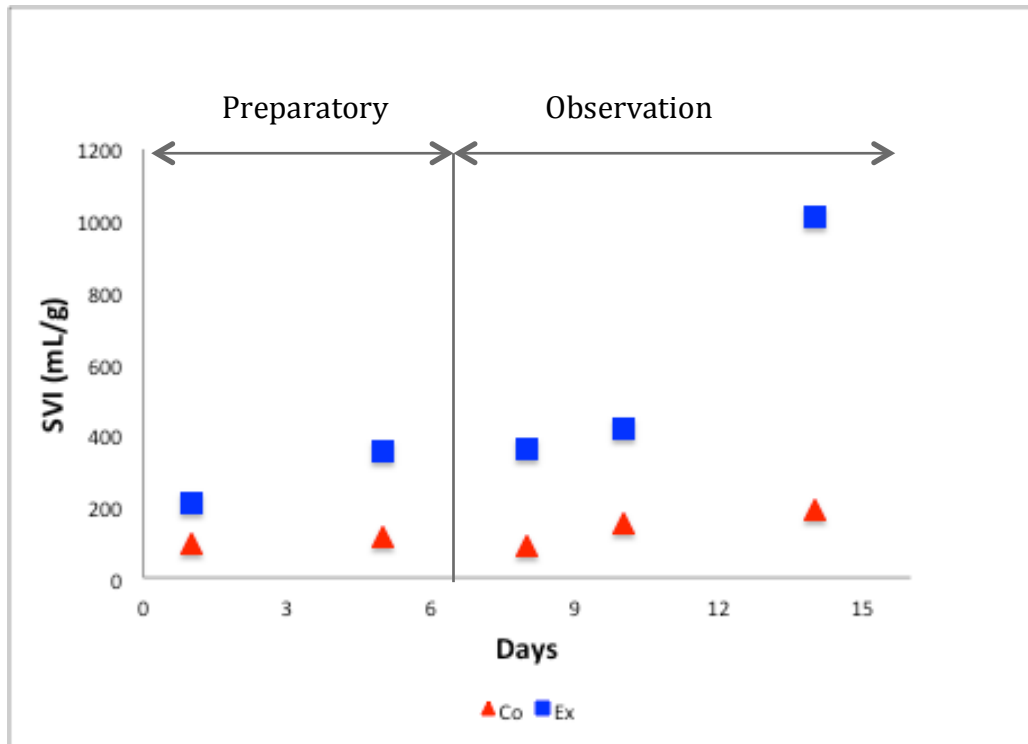


Figure 3.6. Sludge Volume Index (SVI) trend of the control (Co) and experiment (Ex) reactor in Run_B.

In Figure 3.6, experiment reactor SVI was 200 mL/g initially, then increased up to 1000 mL/g nearly which showed significant bulking or huge filamentous organisms growth. Control reactor settling capacity was good which not exceeded than 180 mL/g (APHA 2005). Poor settling leads to biomass washed away by discharge.

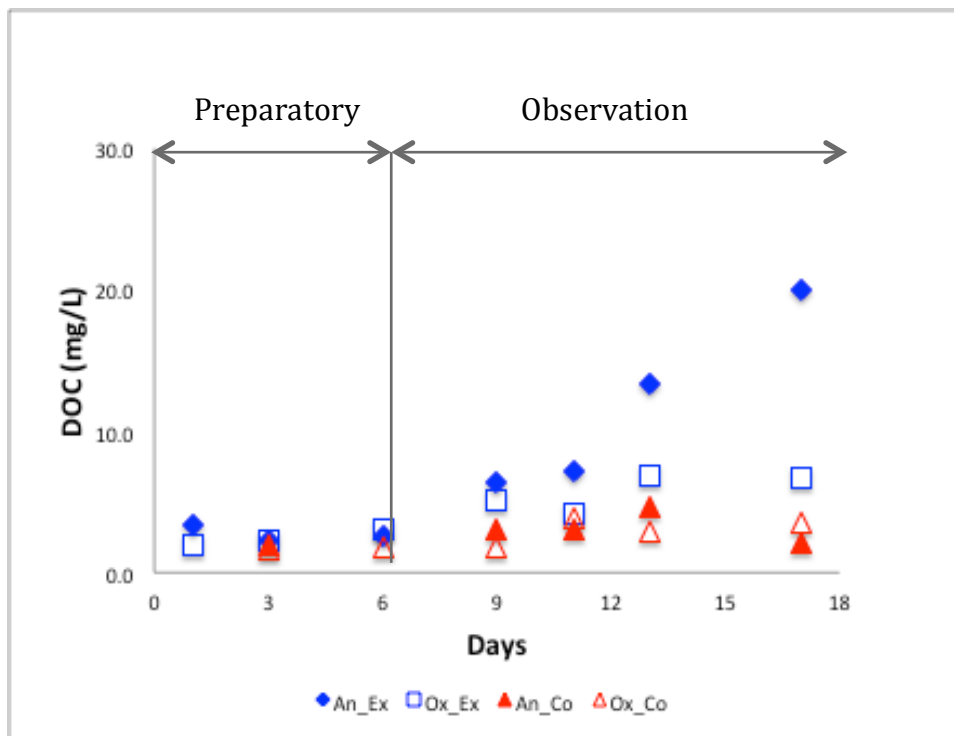


Figure 3.7 DOC concentration of the Run_B.

As shown in Figure 3.7, DOC concentration of the experiment reactor towards to high, which could be the reason of no PAOs who takes VFA in the anaerobic phase. This phenomenon showed deterioration of the experiment reactor condition.

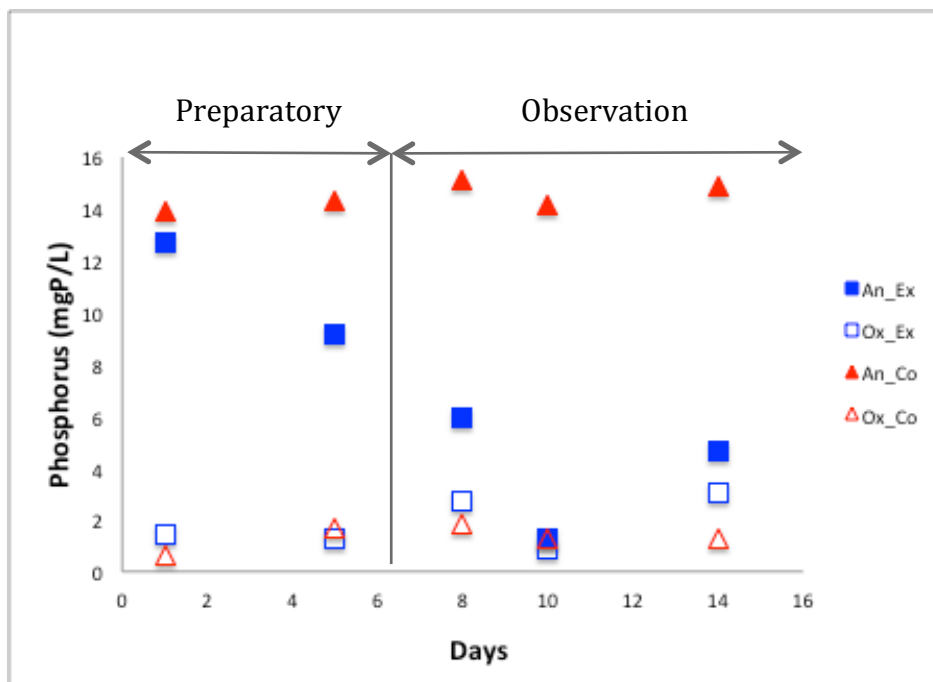


Figure 3.8 Phosphorus concentration in the end of anaerobic (An) and aerobic (Ox) step of experiment (Ex) and control (Co) reactor in Run_B.

As shown in Figure 3.8, experiment reactor P concentration in the end of anaerobic was decreasing, which could be number of PAOs decreased and P release deteriorated in the anaerobic phase. PAOs or bacterial community washed away by discharging due to poor settling.

In total, P removal deterioration in Run_B caused due to filamentous growth and settling ability deteriorated. Then biomass washed away by discharging and resulted poor biomass in the reactor.

Expectation related Fe shortage in this Run_B, are, which bacteria could not grow enough due to Fe shortage and floc could not configured. Because Fe is a growth factor for bacteria, in extend to ion reduction for floc formation (Hanna and Nielsen., 1995).

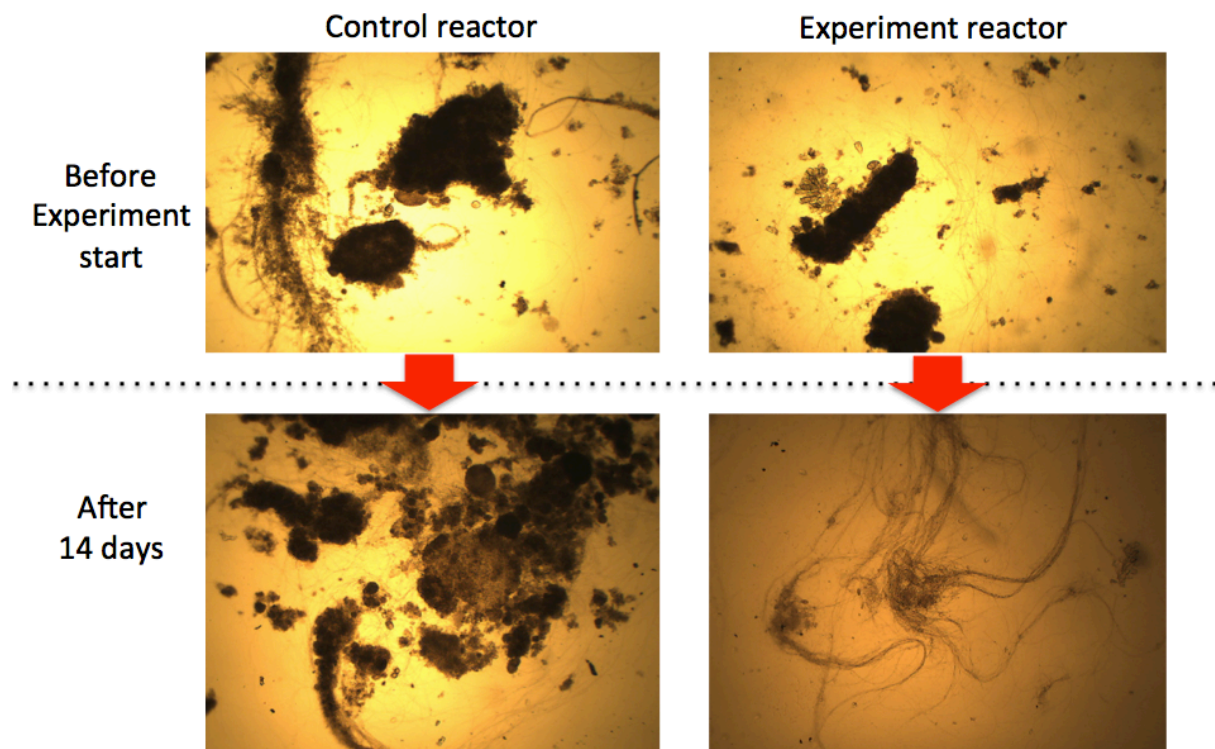


Figure 3.9 Microscope observation of flocculation process in Run_B

In Figure 3.9, showed microscopic observation of the floc in experiment and control reactor of the Run_B. When operation started, two reactors were had similar rich flocculation. After 14 days, control reactor floc increased and had good structure, but experiment reactor flocculation process decreased and showed structure deterioration obviously.

CHAPTER FOUR

Microbial community analyses

In order to clarify the effects of omission of trace elements on EBPR microbial community, samples from Run 8 and Run 10 obtained by Yuki Sato (Sato, 2012), whose master thesis is reviewed in Chapter 2, were analyzed in this chapter by pyrosequencing of partial 16S rRNA and its gene.

DNA and ribosomes were extracted from samples taken and stored by Sato. A partial 16S rRNA gene was amplified by PCR, while a partial 16S rRNA sequence in ribosomes was reverse transcribed and amplified by RT-PCR. Both of the products were further barcoded by PCR with barcoded primers. The barcoded products were pyrosequenced, and the obtained reads were assigned to original samples based on the barcode sequences.

Pyrosequencing of PCR products of 16S rRNA gene (DNA) and RT-PCR products of 16S rRNA (RNA) were expected to give similar results. Yet, DNA is known to be more stable, and PCR products may contain DNA sequences from dead cells. On the other hand, ribosomes are more unstable than DNA, and RT-PCR products would reflect more active cells.

4.1 Materials and Methods

4.1.1 Run8 and Run10 operated by Yuki Sato

Samples from Run8 and Run10 operated and sampled by Mr. Yuki Sato (Sato, 2012) were analyzed.

In both Run8 and Run10, two reactors, a control reactor and an experimental reactor, were operated in parallel, just like Run_A and Run_B in Chapter 3. The operating conditions in

Run8 and Run10 were also the same as in Run_A and Run_B, except for the composition of trace element solution in the influent, and seed sludge.

Seed sludge in Run8 and Run10 were originally from a full scale wastewater treatment plant, which were obtained in **January** 2011. The seed sludge was then acclimatized under the basic operatin conditions as described in Chapter 3, while occasionally experiments to omit some of the trace elements were conducted, as was described in Chapter 2.3. Run8 was conducted during **October 09 – 16 in 2011, and Run 10 November 15 -21, 2011.**

Trace element compositions during the operations were as shown in Table 4.1.

Table 4.1 Trace element concentrations added in the influent, Yuki Sato (2012).

Trace elements	Run8			Run10		
	Preparatory period (Days 1-4)	Comparison period (Days 5-7)		Preparatory period (Days 1-4)	Comparison period (Days 5-7)	
	Both Control and Experimental Reactors (µg/L)	Control Reactor (µg/L)	Experi-mental Reactor (µg/L)	Both Control and Experimental Reactors (µg/L)	Control Reactor (µg/L)	Experi-mental Reactor (µg/L)
Fe	93	93	-	93	93	-
Mo	7.1	7.1	-	7.1	7.1	7.1
Cu	2.3	2.3	2.3	2.3	2.3	-
Co	13	13	13	13	13	-
B	7.9	7.9	-	7.9	7.9	-
I	41	41	-	41	41	-
Mn	10	10	-	10	10	-
Zn	8.2	8.2	-	8.2	8.2	-

The P removal performances of Run8 and Run10 are shown in Fig. 2.5 in Chapter 2 and MLSS, sludge volume index (SVI) and dissolved organic carbon (DOC) concentrations at the end of anaerobic and aerobic phases were shown in the Appendix II.

Samples for microbial community analyses were obtained from the four reactors (a control reactor and an experimental reactor in both Run8 and Run10) for 7 successive days, accounting for a total of 28 samples. The activated sludge mixed liquor samples were taken at the end of the aerobic phase, mixed with pure ethanol (95%) by 1:1 (0.75mL sample + 0.75mL ethanol) and stored at -80°C by Sato.

4.1.2 PCR and Reverse-Transcription PCR (RT-PCR)

In March 2013, the samples stored by Sato were thawed by the author in room temperature, and all samples were sonicated by Advanced Digital Sonifier 250AD cell disrupter (Branson) at an amplitude of 30% (7W) for 10 seconds to extract DNA and ribosomes from cells.

Then samples were diluted 100-fold, and used as the template for PCR and RT-PCR reactions.

Both PCR and RT-PCR were performed targeting V1 through V3 regions of 16S rRNA gene or 16S rRNA using 27f (5'-AGAGTTTGATCMTGGCTCAG-3') and 519r (5'-GWATTACCGCGGCKGCTG-3') primers (Lane 1991). For PCR, ExTaq HotStart Version (Takara, Japan), and for RT-PCR, PrimeScript One Step PCR Kit Version 2 (Takara) were used. The compositions of the 20 μL reaction mixture were as shown below.

PCR mixture/per sample:

10 \times Buffer	2 μL
2.5mM dNTP	1.6 μL
27f primer	0.4 μL
519r primer	0.4 μL
ExTaq Polymerase	0.1 μL
autoclaved Milli-Q	13.5 μL
<u>Template</u>	<u>2 μL</u>
Total:	20 μL

RT-PCR mixture/per sample:

2 \times Buffer	10 μL
RNasin (Promega)	0.4 μL
27f primer	0.8 μL
519r primer	0.8 μL
Enzyme mix	0.8 μL
RNase free H ₂ O	5.2 μL
<u>Template</u>	<u>2 μL</u>
Total	20 μL

As negative control, autoclaved Milli-Q was used as template and subjected to PCR and RT-PCR.

The thermal programs for PCR (30 cycles) and RT-PCR were as below.

PCR: 95°C for 10 min, followed by 30 cycles of 94°C for 30 s, 55.3°C for 30 s, 72°C for 30 s, and a final extension step 72°C for 10 min.

RT-PCR 50°C for 30min, 94°C for 2 min, 20 cycles of 94°C for 30 s, 55.3°C for 30 s, 72°C for 30 s, and a final extension step 72°C for 10 min.

The reactions were performed using a Thermal Cycler Dice (Takara).

After each process, DNA product concentrations were checked by PicoGreen dsDNA Quantification Kit (Invitrogen, USA). To confirm the sizes of the products, products were run on 1% agarose gel by gel electrophoresis in TAE buffer, stained with GelRed (Wako, Japan), and band patterns were visualized in a GelDoc system (BioRad, USA).

4.1.3 Second PCR with barcoded primers

The PCR and RT-PCR products from each sample were further amplified by PCR with barcoded primers so that the PCR products are appended with barcode sequences unique to each sample.

Primers used were as below,

Forward primer: 5'-(adapterA)-(key)-(8base barcode)-(27f) -3'

Reverse primer: 5'-(adapterB)-(key)-519r-3'

where (adapterA) is 5'-CCATCTCATCCCTGCGTGTCTCCGACTCAG-3', (adapterB) is 5'-CCTATCCCCTGTGTGCCTTGGCAGTC-3', (key) is 5'-TCAG-3', (27f) and (519r) are 27f and 519r primer sequences, and (8base barcode) is unique 8 base sequence for each of the samples. The sequences of (adapterA), (adapterB), and (key) are from Roche (2010), 8 base barcode sequences are from the help page of RDP Classifier pyrosequencing pipeline (RDP,

2013), and 27f and 519r primer sequences are from Lane (1991). The primers and sample combinations are listed in Appendix II and Appendix III.

PCR mixture was prepared in the same way as for PCR described in 4.1.2 except that template was PCR or RT-PCR product obtained in 4.1.2, and the number of thermal cycles was 5 but not 30.

The PCR products concentrations were checked by PicoGreen dsDNA Quantification Kit (Invitrogen, USA). The products were grouped into two: one originated from PCR products, and another originated from RT-PCR products from the samples. Each group of samples were mixed together so that the mass of products from each sample is about the same. The quality or the mixtures originated from PCR and RT-PCR products respectively were checked by capillary gel electrophoresis using 2100 Bioanalyzer with a DNA1000 kit (Agilent, USA). A peak with a size around 130bp in addition to the peaks with expected sizes was found in each group. The 130bp peak had to be removed before analysis by pyrosequencing.

To remove the 130bp peaks, for each group, 60 μ L of the mixture was run on 1% low temperature melting agarose gel containing Gel Red (Wako, Japan) (0.5 μ L Gel Red / 20mL gel) in TAE buffer. Gel, which contain expected sized products (600bp) were excised by manual under UV light exposure observation. Then gel slice with DNA products was purified by QIAQuick Gel Extraction kit (Qiagen, USA) according to manufacturer's instruction. Final purified product concentration and quality confirmed by Agilent Bioanalyzer 2100.

Pyrosequencing was done by Center for Omics and Bioinformatics, Department of Computational Biology, Graduate School of Frontier Sciences, The University of Tokyo. Sequencing was done from the AdapterA end.

4.1.4 Pyrosequencing data analysis

Sequence reads were processed basically by the pipeline of QIIME (Caporaso et al., 2010), and visualized by OTUMAMi(Satoh et al., 2012). In splitting process, low quality reads (shorter than 300bp or average quality of reading smaller than 25) were omitted. Operational taxonomic units (OTUs) were formulated by uclust algorithm (Edgar et al., 2010) at 97% similarity. Taxonomic assignments were done by RDP classifier Version 2.2 (Wang et al.,

2007) using GreenGenes 12_10 (97% similarity OTUs) database (McDonald et al., 2012, Werner et al., 2012) as the reference.

OTUMAMi was used for following purposes.

- (a) To prepare data to draw barcharts showing population compositions at different taxonomic levels.
- (b) To prepara heatmaps, and sort the OTUs in the order of phylogenetic tree.
- (c) To prepare FASTA-formatted representative sequences of OTUs of interest.

In (a), Excel (Microsoft, USA) was used to visualize the barcharts.

The FASTA file obtained in (c) was processed by MEGA V5.1 (Tamura et al., 2011) to align the sequences and to calculate phylogenetic trees. Alignment was done by clustalw method (Larkin et al., 2007), and trees were calculated by the neighbor-joining method (Saitou and Nei, 1987) with 1000 bootstrap calculations.

In (b), OTU calculates fraction values and mean fraction values as defined in (1) and (2),

$$f_{i,j} = \left(\frac{c_{i,j}}{\sum_i c_{i,j}} \right) \times 100 \% \quad (1)$$

$$\bar{f}_i = \sum_j f_{i,j} \times \frac{100}{N} \% \quad (2)$$

where $f_{i,j}$ fractions for OTU_j of sample i , \bar{f}_i mean fractions of sample i , $C_{i,j}$ – read counts of OTU j in sample i , and N is total numbers of samples (Sato et al., 2012). Heat maps are generated using the fraction values calculated by (1). And major OTUs can be extracted using the mean fraction values calculated by (2).

To compare microbial population compositions of different samples, mean fraction values for selected OTUs were processed by the Principal Component Analysis (PCA). PCA is a statistical method to compare multivariate data sets. The fraction values related to *Candidatus* “Accumulibacter phosphatis” from the control and experimental reactors by PCR and RT-PCR were used for this analysis. All calculations were done using MarkerView 1.2.1 (ABSciex, USA) version by Pareto scaling.

4.2 Pyrosequencing data result

The numbers of obtained reads for each sample for PCR or RT-PCR were as shown in Table 4.2. The total number of reads obtained was 67,472. The number of reads obtained for each sample for PCR or RT-PCR sample was 1205 in average with a minimum of 548 and a maximum of 1,665.

Table 4.2 Total obtained reads number referred to each days and sample number

Run8															
Experiment reactor								Control reactor							
Sample name	A1	A2	A3	A4	A5	A6	A7	B1	B2	B3	B4	B5	B6	B7	
Total reads	770	777	1506	959	1175	844	891	863	992	1665	1023	941	1025	894	PCR result
Sample name	E1	E2	E3	E4	E5	E6	E7	F1	F2	F3	F4	F5	F6	F7	
Total reads	783	837	798	763	772	1112	821	698	598	935	745	935	769	801	RT-PCR result
	1	2	3	4	5	6	7	1	2	3	4	5	6	7	
	Days							Days							
Run10															
Experiment reactor								Control reactor							
Sample name	C1	C2	C3	C4	C5	C6	C7	D1	D2	D3	D4	D5	D6	D7	
Total reads	801	741	894	1112	1107	986	548	824	993	685	876	1671	1119	747	PCR result
Sample name	G1	G2	G3	G4	G5	G6	G7	H1	H2	H3	H4	H5	H6	H7	
Total reads	778	928	799	886	899	533	812	992	843	757	781	1071	770	844	RT-PCR result
	1	2	3	4	5	6	7	1	2	3	4	5	6	7	
	Days							Days							

Here in this thesis, the author analyzed the reads in the order of taxonomic hierarchical level from higher level to lower. Domain or kingdom level the highest, followed by phylum, class, order, family, genus, and OTU levels. As the OTUs were formulated at 97% similarity levels, and species are often defined by 97% similarities, OTU level here practically means species level.

For example one of OTUs of Candidatus ‘*Accumulibacter phosphatis*’, the assignment result by RDP Classifier with GreenGenes 12_10 (97%) is shown as below.

Root; k_Bacteria; p_Proteobacteria; c_Betaproteobacteria; o_Rhodocyclales; f_Rhodocyclaceae; g_Candidatus Accumulibacter; s__

This means, Root; kingdom – Bacteria, phylum – Proteobacteria, class – Betaproteobacteria, order – Rhodocyclales, family – Rhodocyclaceae, genus - Candidatus Accumulibacter and species level is not determined yet.

4.2.1 Run8

A) Pylum level results

Figure 4.2 shows phylum level read compositions of the PCR and RT-PCR products from Run8. Most dominant bacteria were Proteobacteria.

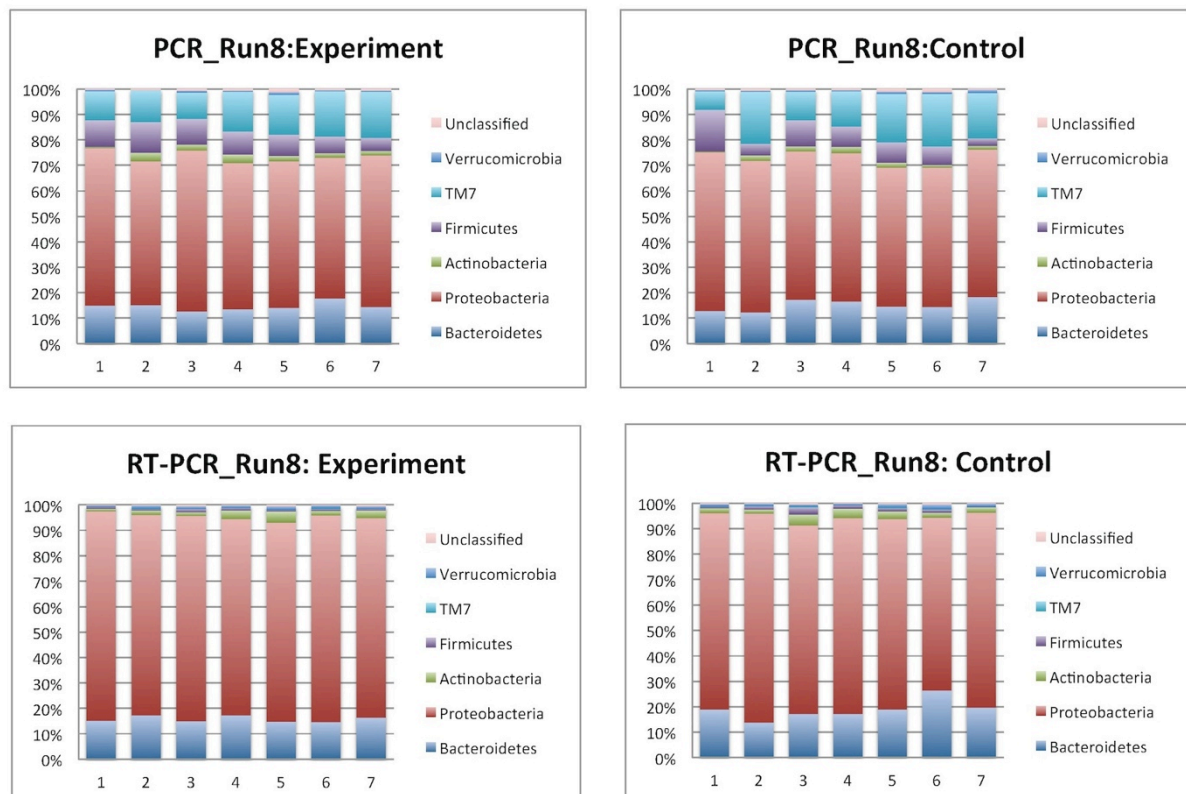


Figure 4.1 Taxonomy assignments of reads at Phylum level of Run8 with PCR and RT-PCR results.

In the PCR result (in the Figure 4.1, upper images), TM7 had significantly high intensity, but in the RT-PCR result (Figure 4.1, lower images) it was practically none in both experiment and control reactor samples. Most of days, Proteobacteria intensity was stable, except 6th day

of RT-PCR result in Control reactor. RT-PCR results are thought to reflect live bacterial cells at the sampling moment. Thus RT-PCR pyrosequencing could be showing more accurate structure of microbial community. But the results of TM7 in RT-PCR cannot directly be accepted, as their DNA was found in the samples with significantly high frequencies. Interestingly, bacterial community of experiment reactor was comparatively stable than control reactor during 7 days.

B) Class level results

At class level, Betaproteobacteria, which is a class under Proteobacteria was dominant (Figure 4.2) in both experiment and control reactor shown in PCR result.

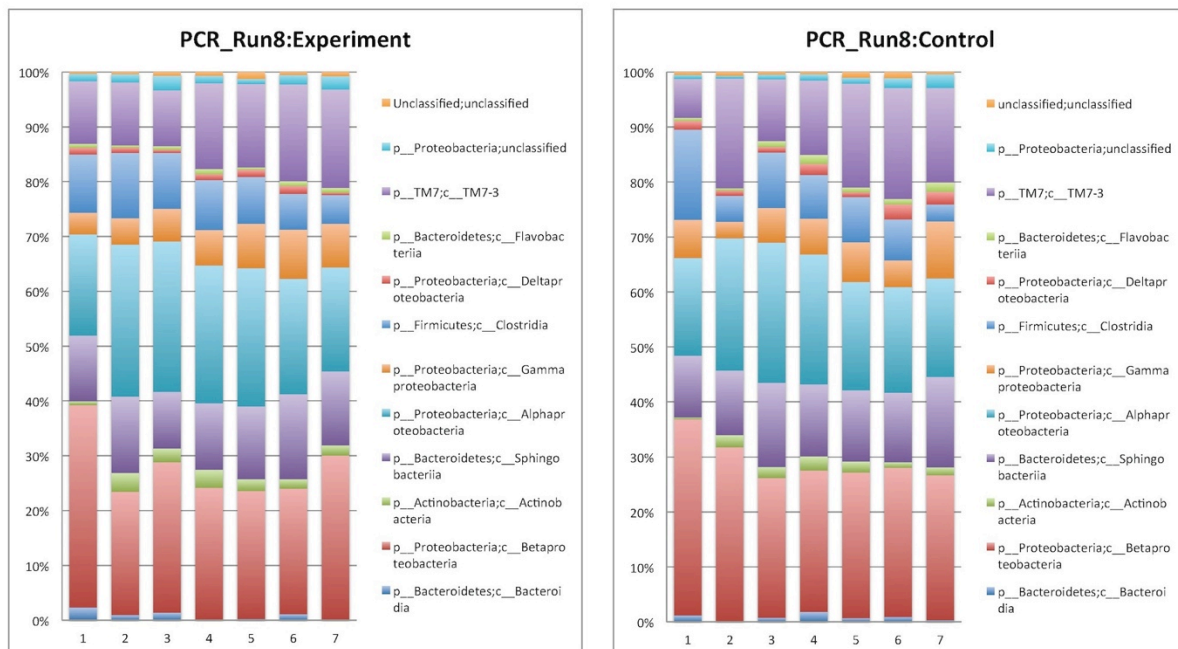


Figure 4.2 Taxonomy assignments of the reads at Class level of PCR results in Run8

Betaproteobacteria trend was stable in control reactor in last 3 days (right image of Figure 4.2). In experiment reactor, initially it was fluctuating, but day4, day5 and day6 were stable, and then increased by little.

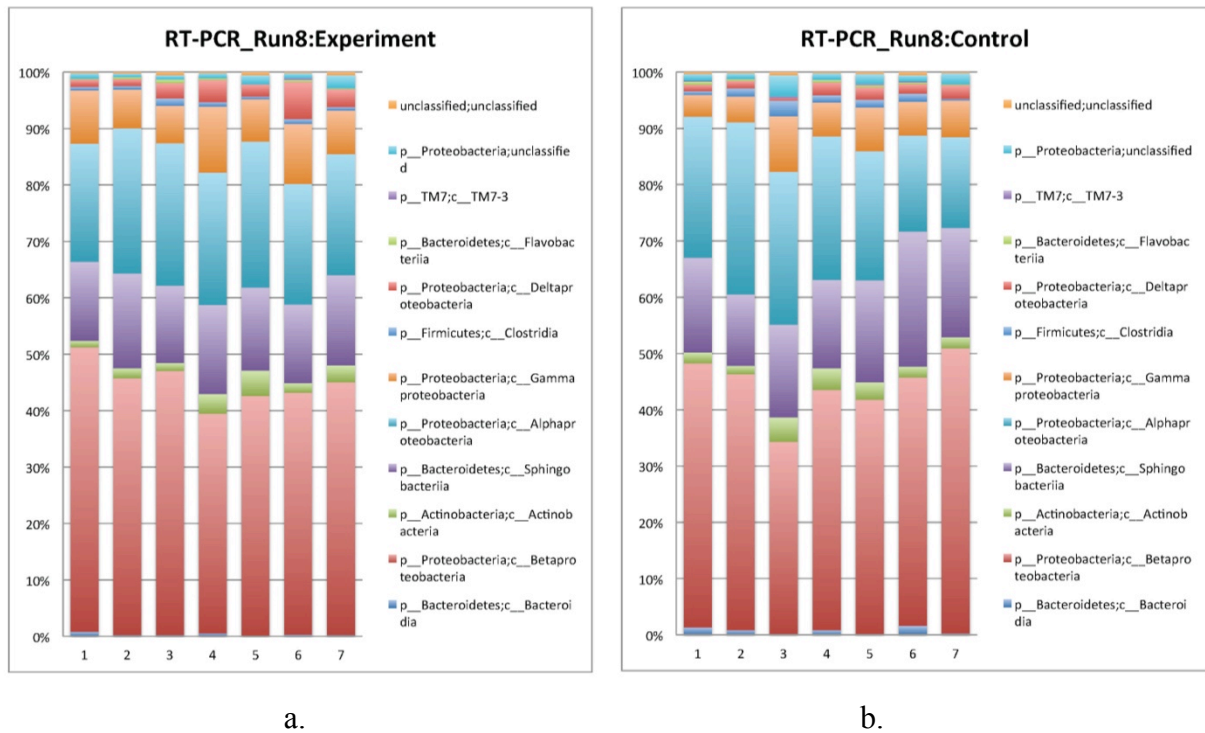


Figure 4.3 Taxonomy assignments of reads at Class level of RT-PCR results in Run8

But in RT-PCR result (Figure 4.3), again, TM7 was not detected in experiment and control reactor. And Betaproteobacteria percentage was higher than PCR result and was more stable during “phosphorus removal deteriorated” period which were 5,6 and 7th day (Figure 4.3 a,b). Deltaproteobacteria was unstable and increased significantly on 6th day of experiment reactor, however it accounted for only a small amount. But it decreased on the last day when total bacterial community structure of the two reactors became similar with each other (Figure 4.3 a.b.).

4.2.2 Run10

A) Pylum level

In the Figure 4.4, PCR and RT-PCR results showed difference obviously. Occupancy by Proteobacteria was more in RT-PCR result due to absence of TM7 (Figure 4.4, lower images), which was observed in the PCR (Figure 4.4 upper images).

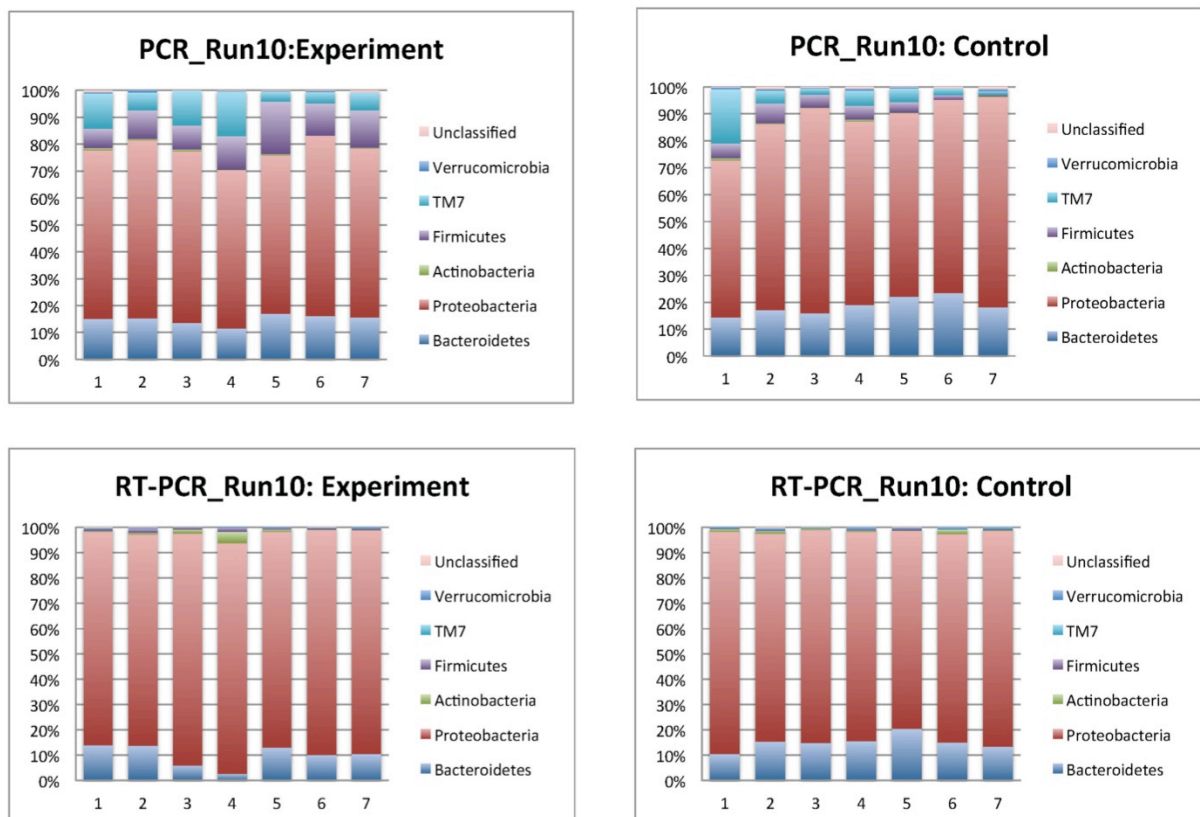


Figure 4.4 Taxonomy assignments of the reads in PCR and RT-PCR result of Run10 in 7 days

B) Class level

Figure 4.5, in the PCR of experiment reactor, TM7 and Firmicutes detected significantly and showed much difference between experiment and control reactor.

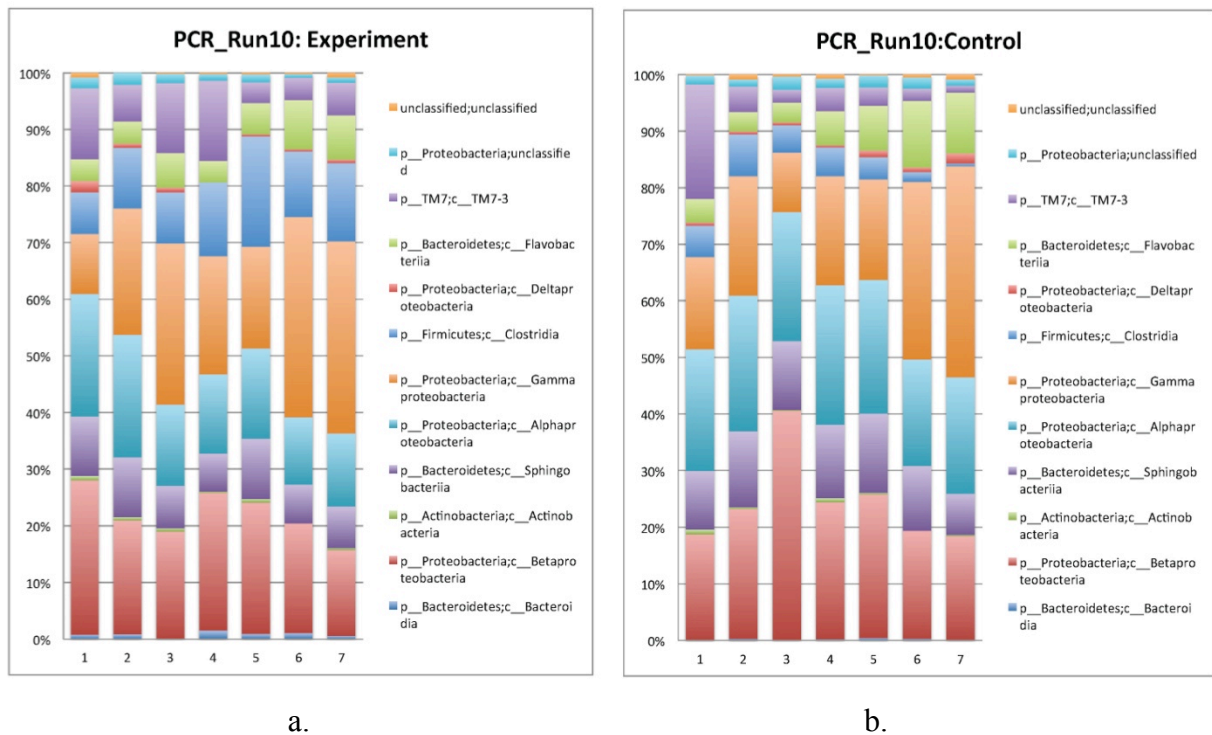


Figure 4.5 Taxonomy assignments of reads in PCR results of Run10

The abundance of Clostridia was apparently different between the two reactors (Figure 4.5, a.b.). Flavobacteria increased gradually in both reactors. TM7 amount in experiment reactor was more than in control reactor and fluctuated remarkably. But in control reactor it decreased gradually.

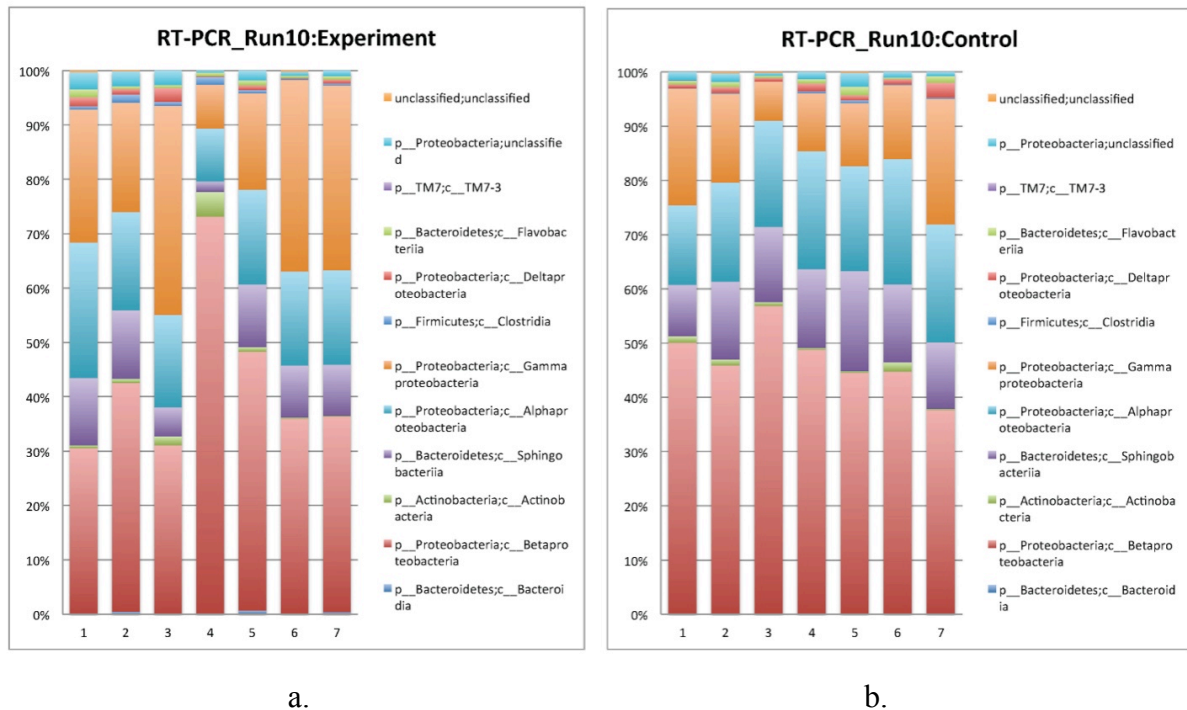


Figure 4.6 Taxonomy assignments of reads in RT-PCR result of Run10

In Figure 4.6, about RT-PCR result, two reactors showed similar structure, except for the 4th day of experiment reactor. In experiment reactor (Figure 4.6 a.), Gammaproteobacteria significantly increased and changed population structure in last two days.

In control reactor (Figure 4.6 b.), Gammaproteobacteria increased gradually. Small amount of Actinobacteria was detected on 6th day. Betaproteobacteria decreased in both of the reactors during experimental stage (day5, 6 and 7), however was more stable in the last two days in experiment reactor.

4.2.3 Operational Taxonomic Units (OTUs) of the Run8 and Run10

The author extracted 41 major OTUs which had average fraction values larger than 0.5%, where the average was calculated for all the 56 samples including those for PCR and RT-PCR. They occupied 63.9% of all OTUs. The fluctuations of their abundances (fraction values) are represented as a heatmap, as shown in Fig. 4.7.

In Fig. 4.7, followings are shown, from left to right.

- A phylogenetic tree showing the phylogenetic relationships between OTUs.
 - The scale bar represents 0.05 substitutions per nucleotide position. Numbers at the nodes are bootstrap values.
- Fourteen columns of a heatmap for Run 8
 - Light color in each cell mean the fraction value for the sample was less. The color is intensified as the fraction value increase.
 - Seven columns on the left are for the experiment reactor, and the other seven columns on the right are for the control reactor.
 - For each column for each OTU, upper cells are showing the fraction values calculated from PCR results, and lower cells from RT-PCR results.
- Next fourteen columns of a heatmap for Run 10
 - Light color in each cell mean the fraction value for the sample was less. The color is intensified as the fraction value increase.
 - Seven columns on the left are for the experiment reactor, and the other seven columns on the right are for the control reactor.
 - For each column for each OTU, upper cells are showing the fraction values calculated from PCR results, and lower cells from RT-PCR results.
- On the rightside of the heatmap are the OTU numbers and their taxonomic assignments.

While PCR results represent bacterial population structure including dead cells, RT-PCR results are thought to represent more active cells. In Fig. 4.7, bacterial population and its change estimated by PCR and RT-PCR are shown.

Figure 4.7 Partial tree and heatmap distribution of major OTUs in Run8 and Run10.

As was shown in Figs 2.5, in both Run8 and Run10, phosphorus removal in the experiment reactors deteriorated during the last 3 days (days 5th, 6th and 7th) right after the omission of selected trace elements in the influent. If the phosphorus removal was caused by the change of bacterial community structure, bacterial community structure on days 5th, 6th and 7th in the experiment reactors should show significant changes from those in the control reactors. But in Figure 4.7, most dominant OTUs between experiment control reactors had no significant differences in both Run8 and Run10.

Alphaproteobacteria related OTU79 was predominant in both Run8 and Run10, but it did not show notable difference between experiment and control reactors. In Run8, it was abundant in both experiment and control reactors. In Run10, it decreased experiment and control reactors simultaneously.

In class Flavobacteria in phylum Bacteroidetes, OTU944 gradually increased in Run10, but it was less in Run8. Similar behavior was observed on OTU703 of *Rheinheimera* sp. But they gradually increased in experiment and control reactor simultaneously, and no clear differences were found during the period when selected trace elements were omitted in the experimental reactors.

Filamentous-type *Thiotrix* sp. was significantly abundant in Run10, however tendency was similar in the experimental and control reactors.

Although, class Sphingobacteria was notably abundant in all the reactors in 2 Runs, they were not affected by the omission of the selected trace elements.

A couple of lineages of polyphosphate accumulating organisms (PAOs) has been reported. The most representative group is classified as *Candidatus* “*Accumulibacter phosphatis*” (*Accumulibacter*), which is in family Rhodocyclaceae in order Rhodocyclales in class Betaproteobacteria in phylum Proteobacteria. They were first reported by Hesselman et al. (1999) as *Rhodocyclus* related bacteria. Some of dominant OTUs in the present study were classified into this group. *Accumulibacter* related OTU288 was predominant in all the reactors in two Runs. The effects of the omission of selected trace elements on *Accumulibacter*-related OTUs will be discussed further in the next section. But the results shown in Fig. 4.8 rather give an impression that *Accumulibacter*-related OTUs were not affected by the omission of the selected trace elements.

Another putative PAOs is *Tetrasphaera* in Actinobacteria phylum level (Beer et al., 2006), but no dominant OTU was found in this group. .

Another important bacterial group in the EBPR system is the glycogen-accumulating organisms (GAOs) which competition with PAOs leads to EBPR deterioration. GAOs are Gammaproteobacteria class (Crocetti et al., 2002), Alphaproteobacteria class (Wong et al., 2004).

While the above observation is the most important outcome that can be seen in Fig. 4.7, the author would like to mention a couple of points which can also be found in Fig. 4.7.

Some of OTUs showed significant differences in PCR and RT-PCR results. Especially, while OTUs in TM7 was detected with high frequencies in DNA, but they were seldom detected in RT-PCR results. This could mean that TM7 cells were not active but still their DNA was present in the reactors anyhow. But such a situation is rather unusual. Another possible explanation is that anyhow rRNA of TM7 could not be amplified. As TM7 has not been reported to be involved in EBPR, in this study, the failure to detect rRNA of TM7 is thought not to be a serious fault. But for microbial community analysis, the reason why TM7 could not be detected in RT-PCR products should be clarified. OTU624 in Clostridia was also seldom detected in RT-PCR products though they were frequently detected in PCR products.

Totally, OTUs which detected in PCR but not detected in RT-PCR, are,

OTU991 – TM7 class

OTU62 – TM7 class

OTU731 – Clostridia

OTU624 – Clostridia

OTU148 – Alphaproteobacteria (showed in one reactor only)

4.2.4 OTUs related to *Candidatus* ‘*Accumulibacter Phosphatis*’

Here, the effect of the omission of trace elements in Run8 and Run10 on OTUs related to *Accumulibacter* is focused. After Hesselmann et al. (1999) reported this species, a numerous number of studies has been conducted on their distribution in different EBPR processes, and their contribution to EBPR. This species distributes around 9-26% in real full-scaled WWTP in worldwide (Zilles et al., 2002a,b, He et al., 2008, Saunders et al., 2003), but dominant in range of 40-90% of lab-scaled EBPR reactor depends on acetate propionate mixed feeding or one of them solely (He et al., 2006, Lu et al., 2006, Pijuan et al., 2004).

The behavior of *Accumulibacter*-related OTUs are extracted from Fig. 4.7 and shown in Fig. 4.8. The sum of the average fractions of four OTUs, OTU288, OTU743, OTU1064 and OTU1547, which are related to *Accumulibacter*, ranged between 0.9 to 11.5%.

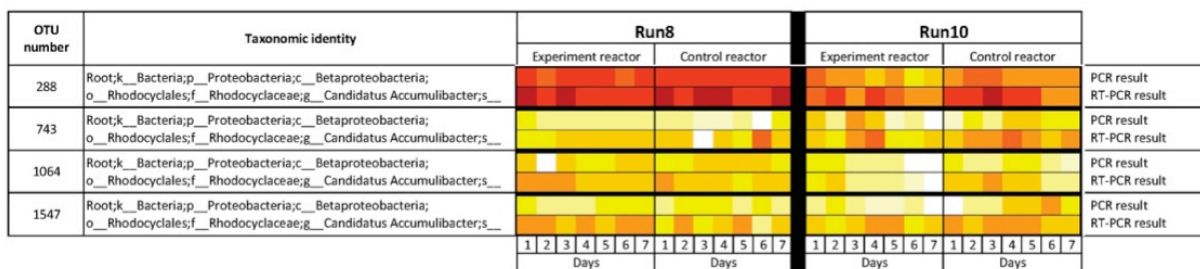


Figure 4. 8 Extraction heatmap of OTUs related to *Candidatus* ‘*Accumulibacter Phosphatis*’

The data shown in Fig. 4.8 were processed by the Principal Component Analysis to see relationship between EBPR deterioration and tendency of these OTUs related to PAO.

Principal Component Analysis is a method to visualize differences of samples which are characterized by a set of multivariate data. The original information in the multivariate data is reduced to a small number of dimensions (principal components) and samples are plotted on axes for each of these dimensions. If samples are plotted closer with each other, these samples are similar, and if their distance increase, then, their differences are bigger.

The results are shown in Fig. 4.9, Fig. 4.10 for Run8 and Fig. 4.11, Fig. 4.12 for Run10. Each figure has a legend at the top, and in the PCA plots, plots of each series are shown by different color line. Angles between each plots vendor are greater than 90⁰C, which indicates they have no significant relationship or plotted close to each other shows some relationship.

	Run8													
	Experiment reactor							Control reactor						
PCR	A1	A2	A3	A4	A5	A6	A7	B1	B2	B3	B4	B5	B6	B7
RT-PCR	E1	E2	E3	E4	E5	E6	E7	F1	F2	F3	F4	F5	F6	F7
Days	1	2	3	4	5	6	7	1	2	3	4	5	6	7

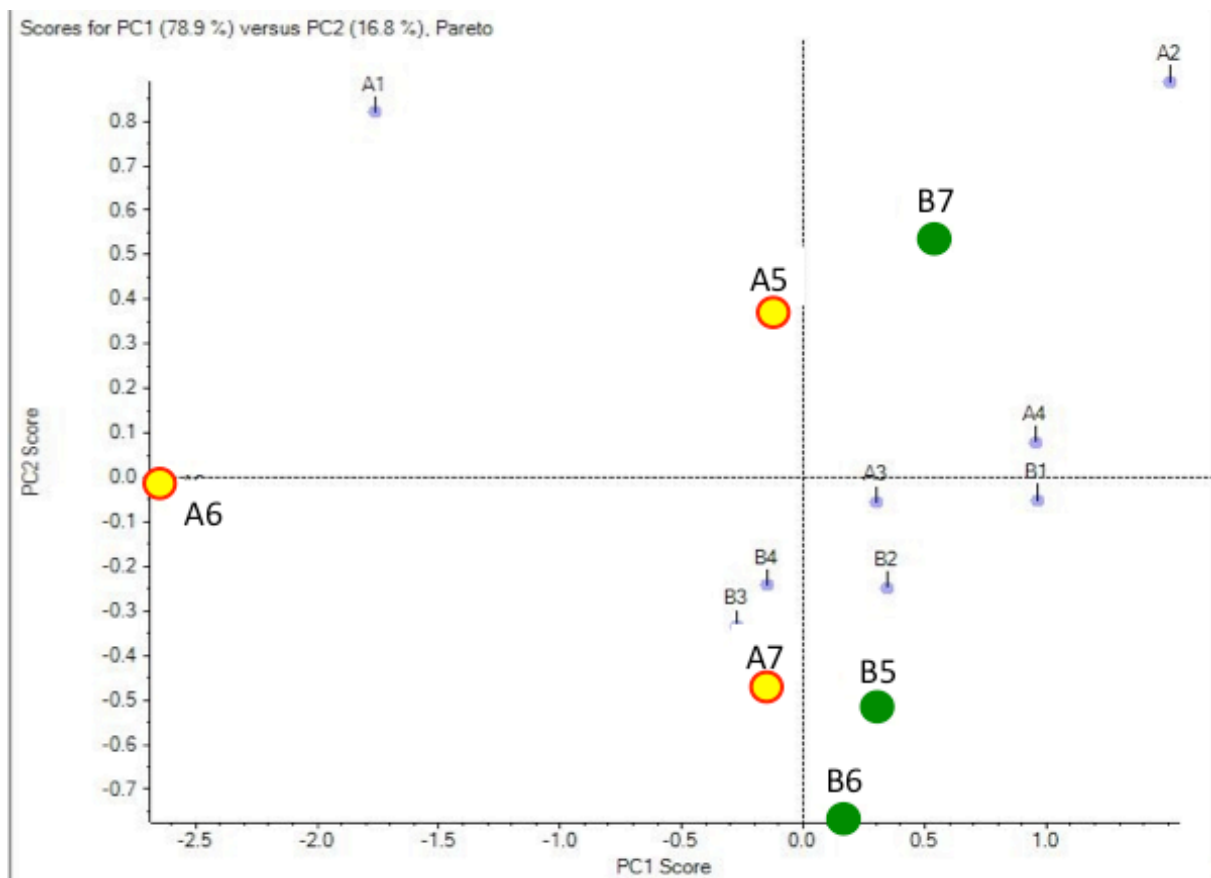


Figure 4.9 2D biplot of *Accumulibacter* related OTUs by PCR results of the Run8 generated by PCA

In Run8 in Fig. 4.9, the plots of A7 and B5, B6, B7 are located close with each other, meaning population of these *Accumulibacter*-related OTUs were similar between the control and the experimental reactors. The position of A6 is distinctly away from A5, A7, B5, B6, and B7. This rather mean that in the experiment reactor, there was some change in *Accumulibacter*-related OTUs on day 6, but it soon changed again and on day 7th, became similar to control reactor.

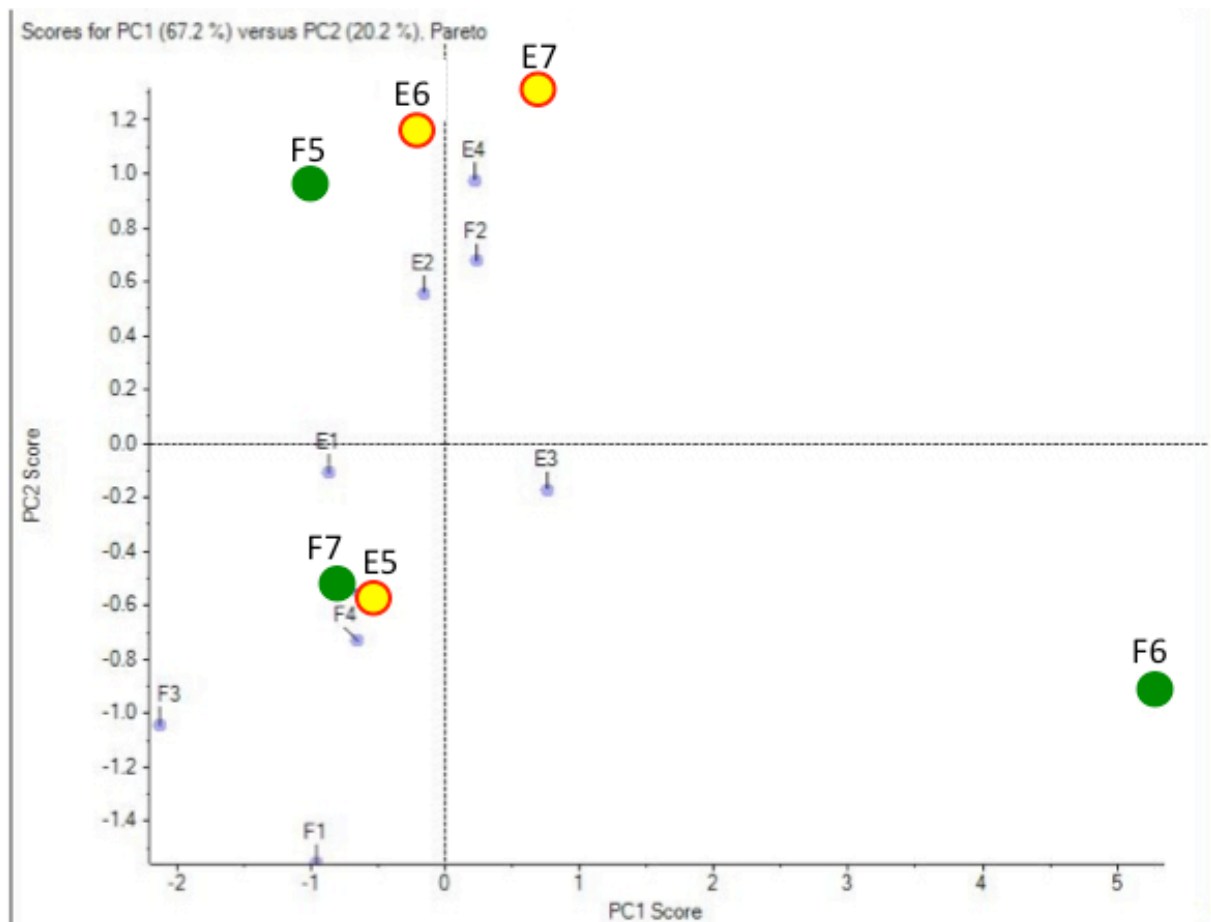


Figure 4.10 2D biplot of *Accumulibacter* related OTUs by RT-PCR results of the Run8 generated by PCA

In Figure 4.10, for RT-PCR, experiment reactor condition was initially in E1 plots, then moved to E2 and E3 plots, back to E4 plots, suddenly changed to E5 plots which similar to control reactor plots F4, F7 and kept stable in E6 and E7. It showed that, experiment reactor condition was naturally unstable regards trace element shortage.

F6, the 5th day in the control reactor was again plotted away from other samples, but came back to close to the plot for F7.

	Run10													
	Experiment reactor							Control reactor						
PCR	C1	C2	C3	C4	C5	C6	C7	D1	D2	D3	D4	D5	D6	D7
RT-PCR	G1	G2	G3	G4	G5	G6	G7	H1	H2	H3	H4	H5	H6	H7
Days	1	2	3	4	5	6	7	1	2	3	4	5	6	7

← Observation plots
← Observation plots

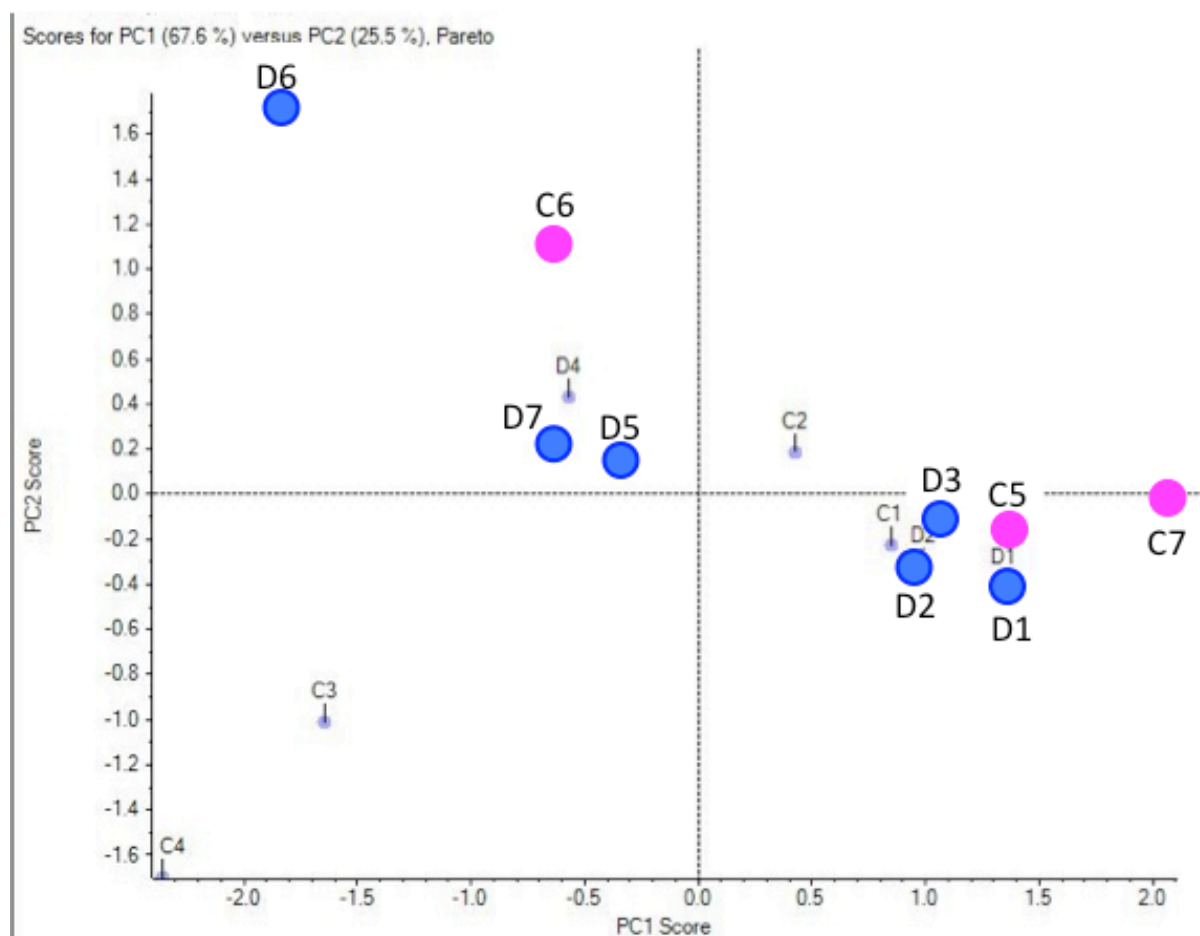


Figure 4.11 2D biplot of *Accumulibacter* related OTUs in PCR result of the Run10 generated by PCA

PCR result of the Run10 showed in Figure 4.11. Experiment reactor condition was in C1 plots, changed to C2, sharply changed to C3, C4 then back to initial condition by C5, but dramatically changed to C6, then back to C7 plots. It means did not create any considerable pattern or relationship, which revealed amongst trace element shortage. Control reactor plots of D4, D5, D6, D7 plotted with experimental reactor C6 and control D1, D2, D3 plotted with experimental C1, C5, and C7, means microbial community change was not related to shortage of trace elements. Thus, experiment reactor data did not show any reflection of trace element shortage.

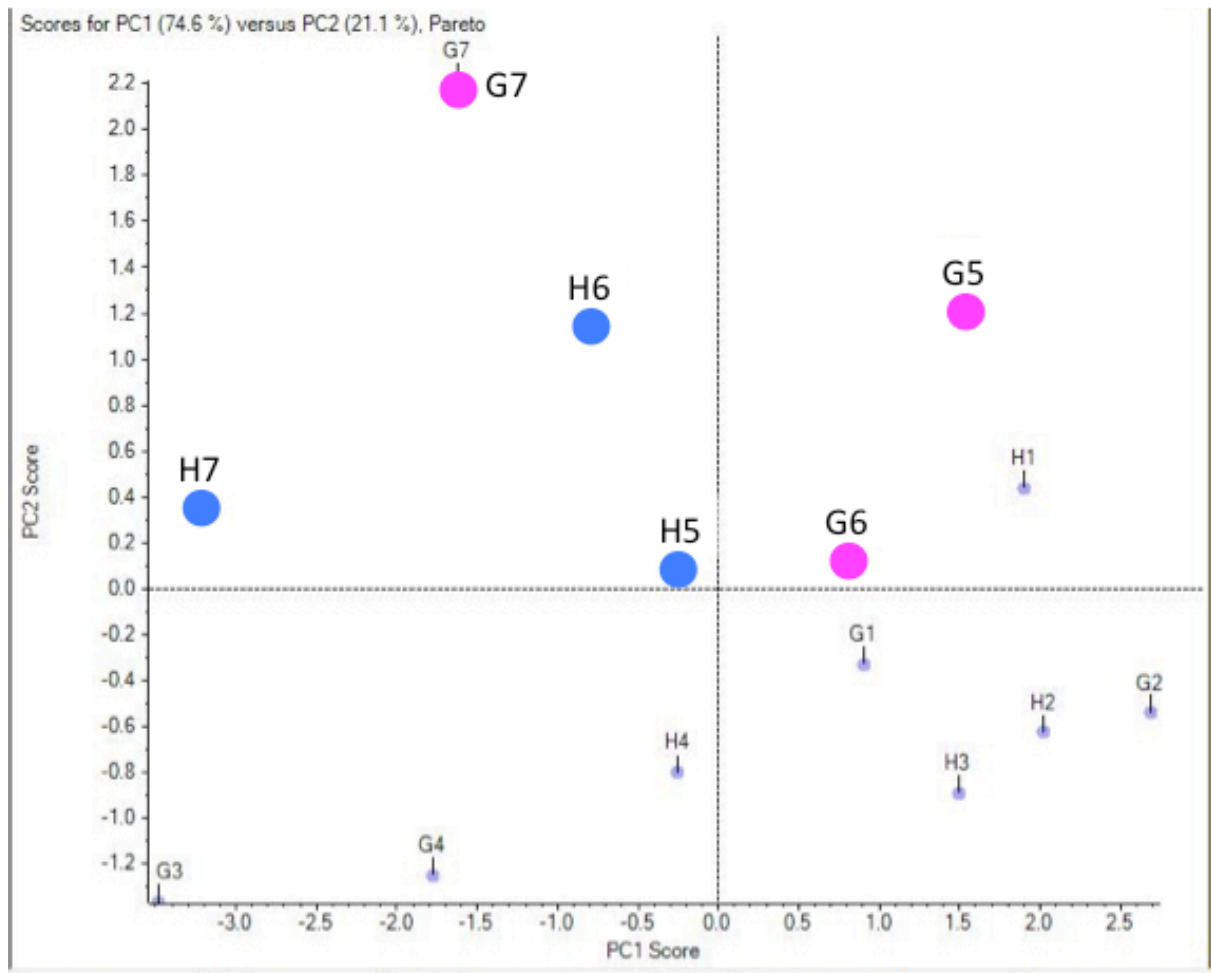


Figure 4.12 2D biplot of *Accumulibacter* related OTUs in RT-PCR result of the Run10 generated by PCA

As shown in Figure 4.12, in RT-PCR result, G series of experiment reactor and H series of control reactor plotted far from each other and could not show any reflection of trace element shortage. Naturally, experiment and control reactor condition was unstable and G5, G6 and G7 did not show a trend.

Accordingly, PCA result did not show significant change related to reactor condition changing (in other words, EBPR deterioration or not deterioration) did not affect to those OTUs.

Pyrosequencing data analyzed from general (phylum and class) level to detailed (OTUs) data in order to discriminate relationship between reactor performance and microbial community change. Based on result, author did not see any significant difference or relationship, which could be reflecting EBPR performance during observation period of under trace element shortage condition.

CHAPTER FIVE

Conclusion and Recommendation

5.1 Conclusion

5.1.1 Reactor operation experiments

The shortage of trace elements affected EBPR in both Run A and Run B. Especially in Run B, the omission of Fe only was demonstrated to caused deterioration of EBPR. In Run_B, filamentous bacteria proliferated after Fe supply was stopped in the experiment reactor, resulted in poor settling, and biomass was washed away by discharge and led to EBPR deterioration.

5.1.2 Microbial community analysis on Run8 and Run10 samples of Yuki Sato

Microbial population change analysis made by pyrosequencing and data analyzed in phylum, class and OTUs levels, which all results showed no significant difference between experiment and control reactor. Accumulibacter-related major OTUs didn't show clear relationship with the deterioration of EBPR.

Apart from EBPR, while DNA (PCR products) and RNA (RT-PCR products) pyrosequencing results were consistent, differences were also found. The most drastic difference was that while TM7 and Clostridia OTUs were detected in PCR, they were seldom detected in RT-PCR.

5.2 Recommendation

5.2.1 Reactor operation experiment

Operate without Fe for a long period: In the present study and in the study done by Sato (2012), effects of omission of trace elements was examined only for a short period of time. And long period experiment would be worth to be done in order to observe any recovery phenomenon or completely deterioration.

5.2.2 Microbial community analysis

Investigate PAOs: PAOs were predominant in the reactor, but EBPR was deteriorated. The question triggered from this phenomenon is “Why PAOs did not work, what impact affected them?”.

Analyze samples of other EBPR deterioration experiments, which caused by trace element shortage: In order to set a full image of relationship between microbial community change and trace elements shortage, further analyze will be recommended on other experiments samples. And confirm reproducibility of present study result would be considered.

Reference:

Journal and Article reference:

- Amann, R.I., Ludwig, W. and Schleifer, K.H. (1995) Phylogenetic identification and in-situ detection of individual microbial cells without cultivation. *Microbiological Reviews*, 59, p.614-623.
- Anderson, I.C., Parkin, P.I. and Campbell, C.D. (2008) DNA- and RNA- derived assessments of fungal community composition in soil amended with sewage sludge rich cadmium, copper and zinc. *Soil Biology & Biochemistry*, 40, p. 2358-2365.
- Bond, P.L., Hugenholtz, P., Keller, J. and Blackall L.L. (1995) Bacterial community structures of phosphate-removing and non-phosphate removing activated sludge from sequencing batch reactors. *Applied and Environmental Microbiology*, 61, p.1910-1916.
- Boon, N., Top, E.M., Verstraete, W. and Siciliano, S.D. (2003) Bioaugmentation as a tool to protect the structure and function of an activated sludge microbial community against a 3-chloroaniline shock load. *Applied and Environmental Microbiology*, 69, p.1511-1520.
- Bowman, M.F., Chambers, P.A., Schindler, D.W.. (2007). Constraints on benthic algal response to nutrient addition in oligotrophic mountain rivers. *River research and applications*, 23(8), p.858-876.
- Burgess, J.E., Quarmby, J. and Stephenson, T. (1999) Role of micronutrients in activated sludge-based biotreatment of industrial effluents. *Biotechnology advances*, 17, p.49-70.
- Burges, J.E., Quarmby, J. and Stephenson, T. (1999) Micronutrient supplements for optimisation of the treatment of industrial wastewater using activated sludge. *Water Research*, 33(18), p. 3707-3714.
- Converti A, Rovatti M, Del Borghi M. (1995) Biological removal of phosphorus from wastewaters by alternating aerobic and anaerobic conditions. *Water Research*, 29(1), p.263-9.
- Crocetti, G.R., Hugenholtz, P., Bond, P.L., Schuler, A., Keller, J., Jenkins, D. and Blackall, L.L. (2000) Identification of polyphosphate-accumulating organisms and design of 16S rRNA-directed probes for their detection and quantitation. *Applied and Environmental Microbiology*, 66, p.1175-1182.
- Edgar, R.C. (2010) Search and clustering orders of magnitude faster than BLAST, *Bioinformatics* 26(19), 2460-2461.
- Fuhs, G.W., and Chen, M. (1975) Microbiological basis of phosphate removal in the activated sludge process for the treatment of wastewater. *Microbial Ecology*, 2(2), p.119-138.

-
- Hanna, R. and Nielsen, P.H. (1996) Iron reduction in activated sludge measured with different extraction techniques. *Water Research*, 30 (3), p.551-558.
- He, S., Gu, A.Z. and McMahon, K.D. (2008) Progress towards understanding the distribution of *Accumulibacter* among full-scale enhanced biological phosphorus removal systems. *Microbial ecology*, 55, p. 229-236.
- Hesselmann, R.P.X., Werlen, C., Hahn, D., van der Meer, J.R., Zehnder, A.J.B. (1999) Enrichment, phylogenetic analysis and detection of a bacterium that performs enhanced biological phosphate removal in activated sludge. *Systematic and Applied Microbiology*, 22(3), p.454-465.
- Hiibel, S.R., Pruden, A., Crimi. B., Reardon. K.R. (2010) Active community profiling via capillary electrophoresis single-strand conformation polymorphism analysis of amplified 16S rRNA and 16S rRNA genes. *Journal of Microbiological Methods*, 83 (2010), p. 286-290.
- Kerkhof, L., and B. B. Ward. (1993) Comparison of nucleic acid hybridization and fluorometry for measurement of the relationship between RNA/DNA ratio and growth rate in a marine bacterium. *Applied Environmental Microbiology*, 59, p.1303–1309.
- Kong, Y.H., Nielsen. J.L. and Nielsen, P.H. (2004) Microautoradiographic study of *Rhodocyclus*-related polyphosphate-accumulating bacteria in full-scale enhanced biological phosphorus removal plants. *Applied and Environmental Microbiology*, 70, p.5383-5390.
- Krishna C. and van Loosdrecht M.C.M. (1999) Effect of temperature on storage polymers and settleability of activated sludge. *Water Research*, 33(10) p.2374– 82.
- Larkin MA, Blackshields G, Brown NP, Chenna R, McGettigan PA, McWilliam H, Valentin F, Wallace IM, Wilm A, Lopez R, Thompson JD, Gibson TJ, Higgins DG. **2007**. Clustal W and Clustal X version 2.0. *Bioinformatics* 23:2947-2948.
- Levin, G.V., and Shapiro, J. (1965). Metabolic uptake of phosphorus by wastewater organisms. *Journal of the Water Pollution Control Federation*. 37, p.800-821.
- Lindrea, K.C. and Seviour, R.J. (2002) Activated sludge – the process. In *Encyclopedia of Environmental Microbiology*. New York, John Wiley and Sons, Inc, p.74-80.
- Liu, W.T., Mino, T., Matsuo, T., Nakamura K. (1996) Biological phosphorus removal process—effect of pH on anaerobic substrate metabolism. *Water Science and Technology*, 34(1– 2), p.25– 32.
- Lu, H.B., Oehmen, A., Viridis, B., Keller, J. and Yuan, Z.G. (2006) Obtaining highly enriched cultures of *Candidatus ‘Accumulibacter phosphatis’* through alternating carbon sources. *Water Research*, 40, p. 3838-3848.
- McDonald D, Price MN, Goodrich J, Nawrocki EP, DeSantis TZ, Probst A, Andersen GL, Knight R, Hugenholtz P. **2012**. An improved Greengenes taxonomy with explicit ranks for ecological and evolutionary analyses of bacteria and archaea. *ISME J* 6(3): 610–618.

-
- Mino T., van Loosdrecht M.C.M. and Heijnen J.J. (1998). Microbiology and biochemistry of the enhanced biological phosphate removal process, *Water research*, 32 (11), p.3193-3207.
- Oehmen, A., P.C. Lemos, G. Garvalho, Z.Yuan, J. Keller, L.L. Blackall, M.A.M. Reis. (2007) Advances in enhanced biological phosphorus removal: From micro to macro scale. *Water Research*. 41, p.2272-2300.
- Pijuan, M., Saunders, A.M., Guisasola, A., Baeza, J.A., Casas, C. and Blackall, L.L. (2004) Enhanced biological phosphorus removal in a sequencing batch reactor using propionate as the sole carbon source. *Biotechnology and Bioengineering*, 85, p. 56-67.
- Roche (2010) GS Junior System Guidelines for Amplicon Experimental Design. 454 Life Sciences Corp. A Roche Company Branford.
- Satoh, H., Mino, T., Matsuo, T., (1992). Uptake of organic substrates and accumulation of polyhydroxyalkanoates linked with glycolysis of intracellular carbohydrates under anaerobic conditions in the biological excess phosphate removal processes. *Water Sci. Technol.* 26 (5-6). P.933-942.
- Satoh, H., Mino, T., Matsuo, T. (1994) Deterioration of enhanced biological phosphorus removal by the domination of microorganisms without polyphosphate accumulation. *Water Science and Technology*, 30(11) p.203 –11.
- Sato, Y. (2012) The study on deterioration of biological phosphorus removal without trace element and specification of short trace element. Master thesis. Socio-cultural Environmental Studies, Graduate School of Frontier Sciences, The University of Tokyo.
- Saunders, A.M., Oehmen, A., Blackall, L.L., Yuan, Z. and Keller, J. (2003) The effect of GAOs (glycogen accumulating organisms) on anaerobic carbon requirements in full-scale Australian EBPR (enhanced biological phosphorus removal) plants. *Water Science and Technology*, 47(11), p.37-43.
- Seviour, R.J., Mino, T., and Onuki, M. (2003) The microbiology of biological phosphorus removal on activated sludge systems. *FEMS Microbiology Reviews*, 27, p.99-127.
- Schuler, A.J. and Jenkins, D. (2003) Enhanced Biological Phosphorus Removal from Wastewater by Biomass with Different Phosphorus content, Part I. Experiment results and comparison with metabolic models. *Water Environment Research*, 75, p.483-498.
- Shehab, O., Deininger, R., Porta, F. and Wojewski, T. (1996) Optimising phosphorus removal at the Ann Arbor wastewater treatment plant. *Water Science and Technology*, 34(1–2), p.493 –439.
- Shendure, J. and Ji, H. (2008) Next-generation DNA sequencing. *Nature Biotechnology*, 26(10), p.1135-1145.
- Srinath E, G., Sastry, C.A. and Pillay, S.C. (1959). Rapid removal of phosphorus from sewage by activated sludge. *Water and Waste treatment*, 11, p.410-415.

-
- Sundblad K, Tonderski A, Rulewski J. Nitrogen and phosphorus in the Vistula river, Poland—changes from source to mouth. *Water Sci Technol* 1994;30(5):177– 86.
- Tamura, K., Peterson, D., Peterson, N., Stecher, G., Nei, M. and Kumar S. (2011) MEGA5: Molecular Evolutionary Genetics Analysis using Maximum Likelihood, Evolutionary Distance, and Maximum Parsimony Methods. *Molecular Biology and Evolution*, 28, p.2731-2739.
- Wang Q, Garrity GM, Tiedje JM, Cole JR. **2007**. Naive Bayesian classifier for rapid assignment of rRNA sequences into the new bacterial taxonomy. *Appl Environ Microb* 73(16): 5261-5267.
- Werner JJ, Koren O, Hugenholtz P, DeSantis TZ, Walters WA, Caporaso JG, Angenent LT, Knight R, Ley RE. **2012**. Impact of training sets on classification of high-throughput bacterial 16S rRNA gene surveys. *ISME J* 6:94-103.
- Zhang, J., Chiodini, R., Badr, A., Zhang, G. (2011) The impact of next-generation sequencing on genomics. *Genetics and Genomics*, 38(2011), p.95-109.
- Zilles, J.L., Hung, C.H. and Noguera, D.R. (2002a) Presence of Rhodocyclus in a full-scale wastewater treatment plant and their participation in enhanced biological phosphorus removal. *Water Science and Technology*, 46(1-2), p.123-128.
- Zilles, J.L., Peccia, J., Kim, M.W., Hung, C.H. and Noguera D.R. (2002b) Involvement of Rhodocyclus-related organisms in phosphorus removal in full-scale wastewater treatment plants. *Applied and Environmental Microbiology*, 68, p.2763-2769.

Book reference

- Gabriel Button. (2011) *Wastewater Microbiology - Fourth edition*. New Jersey, USA: Wiley-Blackwell.
- Metcalf & Eddy. (2004) *Wastewater engineering – Treatment and Reuse*. International edition, Fourth edition: McGraw-Hill Education.
- Michael T. Madigan, John, M. Martinko and Jack Parker. (2009) *Brock biology of microorganisms (12th edition)*. USA: Pearson Education Inc.
- Seviour, Robert and Per H. Nielsen, (2010) *Microbial ecology of Activated Sludge*. London: IWA Publishing.
- Tandoi, V., Jenkins, D., and Warner J. (2006) *Activated sludge Separation Problems*. London: IWA Publishing.

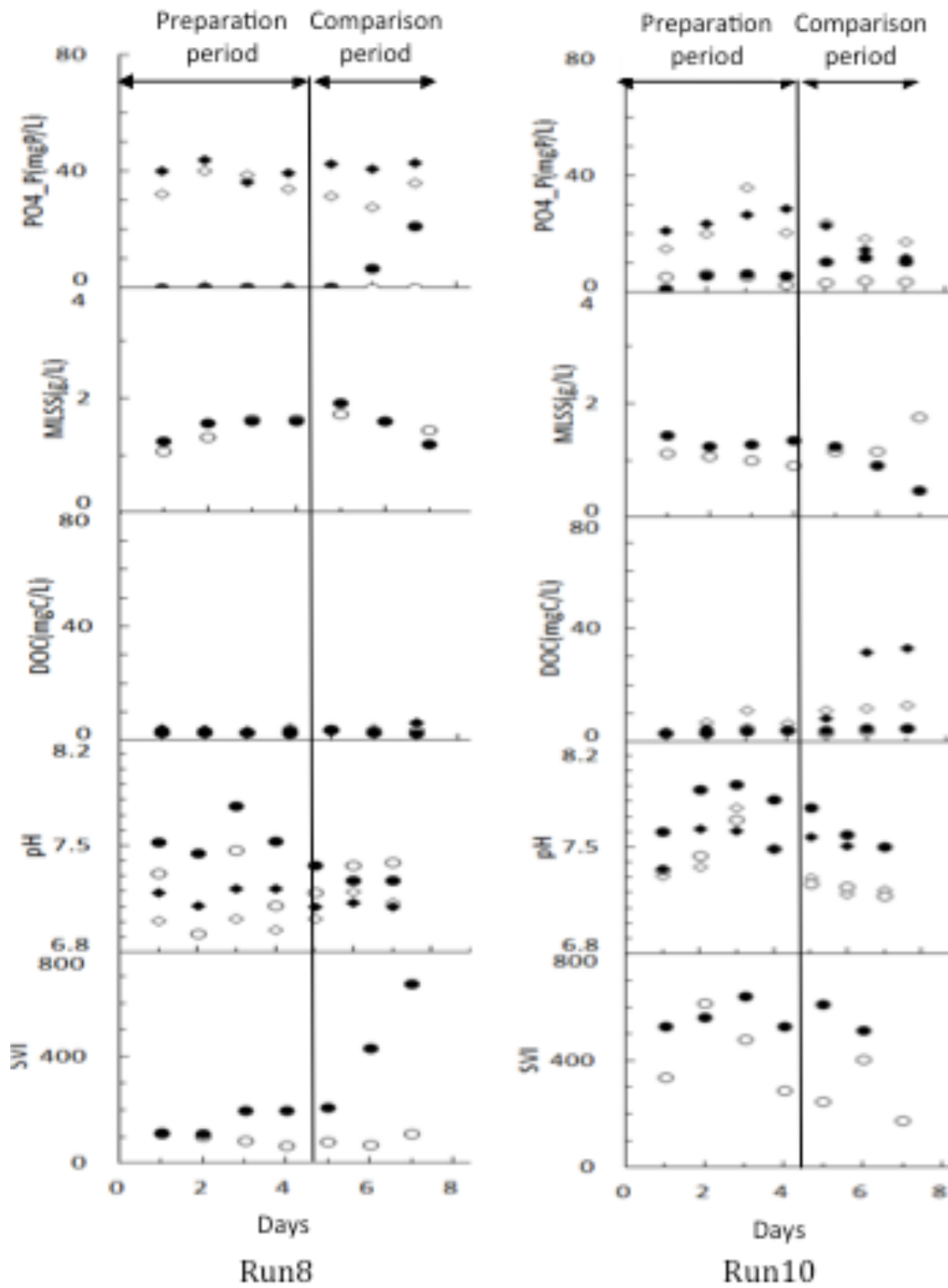
Website reference

- RDP (2013) Pyrosequencing Pipeline Help. Ribosomal Database Project, Center for Microbial Ecology, Michigan State University, USA. (<http://pyro.cme.msu.edu/pyro/help.jsp>)

Appendices

Appendix I

Performance of the Run8 and Run10 conducted by Yuki Sato (Yuki Sato, 2012).



Appendix II

Barcoded primers used in this study

Primer name	Adapter B region	Barcode	519r primer region
519r with adapter	CCTATCCCCTGTGTGCCTTGGCAGTCTCAG	no	GWATTACCGCGG-CKGCTG

Primer name	Adapter A region	Barcode	27f primer region
27f_A1	CCATCTCATCCCTGCGTGTCTCCGACTCAG	AGAGAGAG	AGAGTTTGATCM-TGGCTCAG
27f_A2	CCATCTCATCCCTGCGTGTCTCCGACTCAG	AGAGATGC	AGAGTTTGATCM-TGGCTCAG
27f_A3	CCATCTCATCCCTGCGTGTCTCCGACTCAG	AGAGCAGC	AGAGTTTGATCM-TGGCTCAG
27f_A4	CCATCTCATCCCTGCGTGTCTCCGACTCAG	AGAGCATG	AGAGTTTGATCM-TGGCTCAG
27f_A5	CCATCTCATCCCTGCGTGTCTCCGACTCAG	AGATCATC	AGAGTTTGATCM-TGGCTCAG
27f_A6	CCATCTCATCCCTGCGTGTCTCCGACTCAG	AGATCTGC	AGAGTTTGATCM-TGGCTCAG
27f_A7	CCATCTCATCCCTGCGTGTCTCCGACTCAG	AGATGAGC	AGAGTTTGATCM-TGGCTCAG
27f_B1	CCATCTCATCCCTGCGTGTCTCCGACTCAG	AGATGCAG	AGAGTTTGATCM-TGGCTCAG
27f_B2	CCATCTCATCCCTGCGTGTCTCCGACTCAG	AGATGCTC	AGAGTTTGATCM-TGGCTCAG
27f_B3	CCATCTCATCCCTGCGTGTCTCCGACTCAG	AGCAGAGC	AGAGTTTGATCM-TGGCTCAG
27f_B4	CCATCTCATCCCTGCGTGTCTCCGACTCAG	AGCAGATG	AGAGTTTGATCM-TGGCTCAG
27f_B5	CCATCTCATCCCTGCGTGTCTCCGACTCAG	AGCAGCAG	AGAGTTTGATCM-TGGCTCAG
27f_B6	CCATCTCATCCCTGCGTGTCTCCGACTCAG	AGCAGCTC	AGAGTTTGATCM-TGGCTCAG
27f_B7	CCATCTCATCCCTGCGTGTCTCCGACTCAG	AGCATCTG	AGAGTTTGATCM-TGGCTCAG
27f_C1	CCATCTCATCCCTGCGTGTCTCCGACTCAG	AGCTCAGC	AGAGTTTGATCM-TGGCTCAG
27f_C2	CCATCTCATCCCTGCGTGTCTCCGACTCAG	AGCTCATG	AGAGTTTGATCM-TGGCTCAG
27f_C3	CCATCTCATCCCTGCGTGTCTCCGACTCAG	AGCTGATC	AGAGTTTGATCM-TGGCTCAG
27f_C4	CCATCTCATCCCTGCGTGTCTCCGACTCAG	AGCTGCTG	AGAGTTTGATCM-TGGCTCAG
27f_C5	CCATCTCATCCCTGCGTGTCTCCGACTCAG	ATCAGATC	AGAGTTTGATCM-TGGCTCAG
27f_C6	CCATCTCATCCCTGCGTGTCTCCGACTCAG	ATCAGCTG	AGAGTTTGATCM-TGGCTCAG
27f_C7	CCATCTCATCCCTGCGTGTCTCCGACTCAG	ATCATCAG	AGAGTTTGATCM-TGGCTCAG
27f_D1	CCATCTCATCCCTGCGTGTCTCCGACTCAG	ATCTCATC	AGAGTTTGATCM-TGGCTCAG
27f_D2	CCATCTCATCCCTGCGTGTCTCCGACTCAG	ATCTCTGC	AGAGTTTGATCM-TGGCTCAG
27f_D4	CCATCTCATCCCTGCGTGTCTCCGACTCAG	ATCTGATG	AGAGTTTGATCM-TGGCTCAG
27f_D5	CCATCTCATCCCTGCGTGTCTCCGACTCAG	ATCTGCAG	AGAGTTTGATCM-TGGCTCAG
27f_D6	CCATCTCATCCCTGCGTGTCTCCGACTCAG	ATCTGCTC	AGAGTTTGATCM-TGGCTCAG
27f_D7	CCATCTCATCCCTGCGTGTCTCCGACTCAG	ATGAGAGC	AGAGTTTGATCM-TGGCTCAG
27f_D8	CCATCTCATCCCTGCGTGTCTCCGACTCAG	ATGAGATG	AGAGTTTGATCM-TGGCTCAG
27f_E1	CCATCTCATCCCTGCGTGTCTCCGACTCAG	ATGAGCAG	AGAGTTTGATCM-TGGCTCAG
27f_E2	CCATCTCATCCCTGCGTGTCTCCGACTCAG	ATGAGCTC	AGAGTTTGATCM-TGGCTCAG
27f_E3	CCATCTCATCCCTGCGTGTCTCCGACTCAG	ATGATCTG	AGAGTTTGATCM-TGGCTCAG
27f_E4	CCATCTCATCCCTGCGTGTCTCCGACTCAG	ATGATGAG	AGAGTTTGATCM-TGGCTCAG

Continue

Primer name	Adapter A region	Barcode	27f primer region
27f_E5	CCATCTCATCCCTGCGTGTCTCCGACTCAG	ATGCAGAG	AGAGTTTGATCM-TGGCTCAG
27f_E6	CCATCTCATCCCTGCGTGTCTCCGACTCAG	ATGCATGC	AGAGTTTGATCM-TGGCTCAG
27f_E7	CCATCTCATCCCTGCGTGTCTCCGACTCAG	ATGCTCAG	AGAGTTTGATCM-TGGCTCAG
27f_F1	CCATCTCATCCCTGCGTGTCTCCGACTCAG	CAGAGAGC	AGAGTTTGATCM-TGGCTCAG
27f_F2	CCATCTCATCCCTGCGTGTCTCCGACTCAG	CAGAGATG	AGAGTTTGATCM-TGGCTCAG
27f_F3	CCATCTCATCCCTGCGTGTCTCCGACTCAG	CAGAGCAG	AGAGTTTGATCM-TGGCTCAG
27f_F4	CCATCTCATCCCTGCGTGTCTCCGACTCAG	CAGAGCTC	AGAGTTTGATCM-TGGCTCAG
27f_F5	CCATCTCATCCCTGCGTGTCTCCGACTCAG	CAGATCTG	AGAGTTTGATCM-TGGCTCAG
27f_F6	CCATCTCATCCCTGCGTGTCTCCGACTCAG	CAGATGAG	AGAGTTTGATCM-TGGCTCAG
27f_F7	CCATCTCATCCCTGCGTGTCTCCGACTCAG	CAGCAGAG	AGAGTTTGATCM-TGGCTCAG
27f_G1	CCATCTCATCCCTGCGTGTCTCCGACTCAG	CAGCTCAG	AGAGTTTGATCM-TGGCTCAG
27f_G2	CCATCTCATCCCTGCGTGTCTCCGACTCAG	CAGCTCTC	AGAGTTTGATCM-TGGCTCAG
27f_G3	CCATCTCATCCCTGCGTGTCTCCGACTCAG	CATCTCTG	AGAGTTTGATCM-TGGCTCAG
27f_G4	CCATCTCATCCCTGCGTGTCTCCGACTCAG	CATCTGAG	AGAGTTTGATCM-TGGCTCAG
27f_G5	CCATCTCATCCCTGCGTGTCTCCGACTCAG	CATGAGAG	AGAGTTTGATCM-TGGCTCAG
27f_G6	CCATCTCATCCCTGCGTGTCTCCGACTCAG	CATGATGC	AGAGTTTGATCM-TGGCTCAG
27f_G7	CCATCTCATCCCTGCGTGTCTCCGACTCAG	CATGCAGC	AGAGTTTGATCM-TGGCTCAG
27f_H1	CCATCTCATCCCTGCGTGTCTCCGACTCAG	CTCAGAGC	AGAGTTTGATCM-TGGCTCAG
27f_H2	CCATCTCATCCCTGCGTGTCTCCGACTCAG	CTCAGATG	AGAGTTTGATCM-TGGCTCAG
27f_H3	CCATCTCATCCCTGCGTGTCTCCGACTCAG	CTCAGCAG	AGAGTTTGATCM-TGGCTCAG
27f_H4	CCATCTCATCCCTGCGTGTCTCCGACTCAG	CTCAGCTC	AGAGTTTGATCM-TGGCTCAG
27f_H5	CCATCTCATCCCTGCGTGTCTCCGACTCAG	CTCATCTG	AGAGTTTGATCM-TGGCTCAG
27f_H6	CCATCTCATCCCTGCGTGTCTCCGACTCAG	CTCATGAG	AGAGTTTGATCM-TGGCTCAG
27f_H7	CCATCTCATCCCTGCGTGTCTCCGACTCAG	CTCTCAGC	AGAGTTTGATCM-TGGCTCAG

Appendix III

Barcoded primers assigned to numbers

Products		1	2	3	4	5	6	7	8	Run	Reactor
PCR	A	A1	A2	A3	A4	A5	A6	A7	-	Run8	Experiment
	B	B1	B2	B3	B4	B5	B6	B7	-		Control
	C	C1	C2	C3	C4	C5	C6	C7	-	Run10	Experiment
	D	D1	D2	X	D3	D4	D5	D6	D7		Control
RT-PCR	E	E1	E2	E3	E4	E5	E6	E7	-	Run8	Experiment
	F	F1	F2	F3	F4	F5	F6	F7	-		Control
	G	G1	G2	G3	G4	G5	G6	G7	-	Run10	Experiment
	H	H1	H2	H3	H4	H5	H6	H7	-		Control
J	-	-	-	X	-	-	-	-	-		

Sample distribution in primers location

Products		1	2	3	4	5	6	7	8	Run	Reactor
PCR	A	9-Oct	11-Oct	12-Oct	13-Oct	14-Oct	15-Oct	16-Oct	-	Run8	Experiment
	B	9-Oct	11-Oct	12-Oct	13-Oct	14-Oct	15-Oct	16-Oct	-		Control
	C	15-Nov	16-Nov	17-Nov	18-Nov	19-Nov	20-Nov	21-Nov	-	Run10	Experiment
	D	15-Nov	16-Nov	X	17-Nov	18-Nov	19-Nov	20-Nov	21-Nov		Control
RT-PCR	E	9-Oct	11-Oct	12-Oct	13-Oct	14-Oct	15-Oct	16-Oct	-	Run8	Experiment
	F	9-Oct	11-Oct	12-Oct	13-Oct	14-Oct	15-Oct	16-Oct	-		Control
	G	15-Nov	16-Nov	17-Nov	18-Nov	19-Nov	20-Nov	21-Nov	-	Run10	Experiment
	H	15-Nov	16-Nov	17-Nov	18-Nov	19-Nov	20-Nov	21-Nov	-		Control
J	-	-	-	X	-	-	-	-	-		